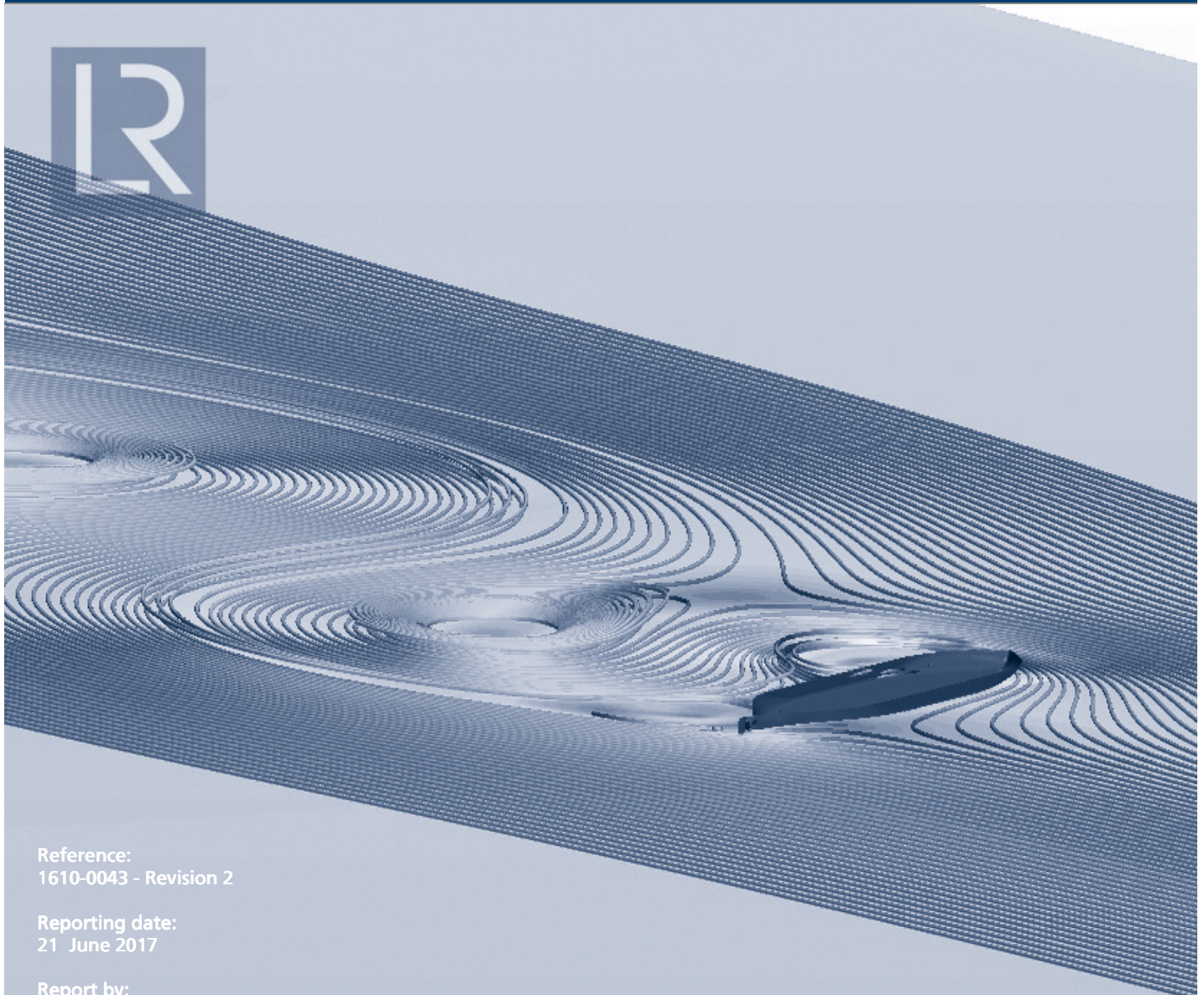


OCIMF

CFD current drag

Technical Investigation Department

Report for:
MEG 4 Working Group



Reference:
1610-0043 - Revision 2

Reporting date:
21 June 2017

Report by:
Erik A.J. Vroegrijk, Technical Investigation Department

Front cover: Streamlines generated by 150kDWT Post Marpol tanker at ballast draught, WD/T 1.02 and 60 degrees, using free sink and trim.

The contents of this report are for the confidential information of the client and members of the Lloyd's Register Group.

Report summary

At the request of the MEG 4 Working Group from Oil Companies International Marine Forum (OCIMF), the undersigned Specialist to Lloyd's Register EMEA's Technical Investigation Department (TID) calculated the current drag coefficients for various sized tankers and an LNG carrier using viscous Computational Fluid Dynamic (CFD). The main objective of this work was to produce CFD derived current coefficients, to be published in the fourth edition of the Mooring Equipment Guidelines (MEG).

The original current coefficients, published in [1], were derived by model tests conducted in the 1970's and 1990's using Pre Marpol tankers. Initially, Lloyd's Register EMEA was contracted to study the applicability of these curves to Post Marpol tankers, which typically feature a wider beam. The results, reported in [2], showed no substantial difference between current forces experienced by Pre- and Post Marpol tankers. It further indicated that the published curves were conservative, especially for the lower water depth to draught (Wd/T) ratios and beam-on current. A study published by MARIN [3] indicated that tank blockage effects could have resulted in the higher, more conservative, force coefficients in the OCIMF publication.

The scope of work presented in this report consisted of four parts. The first part benchmarked LR's CFD capabilities against MARIN's [3], by studying a similar sized LNG carrier at model scale. The second part considered the development of the current curves for four Wd/T ratios, using the 150kDWT Post Marpol tanker from [2]. This part also included a study on the effects of vessel size by comparing results for 50kDWT, 150kDWT and 300kDWT tankers for a select number of conditions. Thirdly, the applicability of the current curves to LNG vessels was investigated. The last part investigated the effect of current velocity on the curves, using the 50kDWT tanker. The remainder of this report is structured in-line with these parts.

Based on the results and discussion, the following conclusions can be drawn:

- LR CFD results compare well with equivalent calculations conducted by MARIN in [3].
- Current coefficients for free sink and trim can be closely approximated by applying the dynamic Wd/T ratio, which takes into account sinkage, to the curves derived from fixed CFD calculations.
- The current coefficients are shown to be marginal sensitivity to vessel size and shape, with the sharper form resulting generally in larger forces.
- The CFD derived current curves could be applied to LNG Carriers if an additional safety margin is applied to scenarios with low Wd/T ratios.
- The current coefficients are only marginally sensitive to the current speed, due to relative changes in the dynamic floating position. This sensitivity is in the same order as the sensitivity to hull shape, which can be up to 10%.

The following recommendations are made:

- Calculate the force coefficients at Wd/T 1.00 on both laden and ballast draught to verify they converge to the same values.
- Calculate the force coefficients at Wd/T 1.50 on laden draught to allow for a smoother transition between the CFD derived curves at the same angle of current incidence.

Written by:	Approved by:
Erik A.J. Vroegrijk, MSc.	Chris Craddock, PhD., BEng.
Signature:	Signature:
	
Designation:	Designation:
Specialist Hydrodynamics	Fluid Dynamics Manager
Date of approval:	
21 June 2017	

Contents

Summary	i
1. Introduction	4
2. Methodology	4
2.1 Benchmark LNG	4
2.2 Full curve development	5
2.3 LNG carrier	5
2.4 Current sensitivity	5
3. Results	6
3.1 Benchmark LNG	6
3.2 Full curve development	6
3.3 LNG carrier	7
3.4 Current sensitivity	7
4. Discussion	8
4.1 Benchmark LNG	8
4.2 Full curve development	8
4.3 LNG Carrier	9
4.4 Current sensitivity	9
5. Conclusions	10
6. Recommendations	10
7. References	10
Tables	11
Figures	15

1. Introduction

At the request of the MEG 4 Working Group from Oil Companies International Marine Forum (OCIMF), the undersigned Specialist to Lloyd's Register EMEA's Technical Investigation Department (TID) calculated the current drag coefficients for various sized tankers and an LNG carrier using viscous Computational Fluid Dynamic (CFD). The main objective of this work was to produce CFD derived current coefficients, to be published in the fourth edition of the Mooring Equipment Guidelines (MEG).

The original current coefficients, published in [1], were derived by model tests conducted in the 1970's and 1990's using Pre Marpol tankers. Initially, Lloyd's Register EMEA was contracted to study the applicability of these curves to Post Marpol tankers, which typically feature a wider beam. The results, reported in [2], showed no substantial difference between current forces experienced by Pre- and Post Marpol tankers. It further indicated that the published curves were conservative, especially for the lower water depth to draught (Wd/T) ratios and beam-on current. A study published by MARIN [3] indicated that tank blockage effects could have resulted in the higher, more conservative, force coefficients in the OCIMF publication.

The scope of work presented in this report consisted of four parts. The first part benchmarked LR's CFD capabilities against MARIN's [3], by studying a similar sized LNG carrier at model scale. The second part considered the development of the current curves for four Wd/T ratios, using the 150kDWT Post Marpol tanker from [2]. This part also included a study on the effects of vessel size by comparing results for 50kDWT, 150kDWT and 300kDWT tankers for a select number of conditions. In this revised report (1610-0043 Report 1v3), the head-on and stern-on current conditions have been included. Thirdly, the applicability of the current curves to LNG vessels was investigated. The last part investigated the effect of current velocity on the curves, using the 50kDWT tanker. The remainder of this report is structured in-line with these parts.

2. Methodology

The computational method used in this study is identical to the one used for calculating Free Sink and Trim (FST) cases in the TID7796C – Revision 1 [2] report. Given that [2] contains a detailed description of the simulation setup, it suffices to summarise the most important aspects here.

All simulations applied the Reynolds Averaged Navier-Stokes Equations (RANSE) CFD model, in which the ship and the surroundings seas were modelled using a Double Body (DB) approach. Previous calculations in [2] and independent calculations in [3] confirmed that free surface effects can be considered negligible. The k- ω SST turbulence model was selected and a wall functions approach applied, targeting a mean y^+ value of around 200.

Apart from the benchmark study, all simulations used the 1/7 power law to mimic the natural current flow profile through the water depth. Free Sink and Trim was in all cases modelled using a quasi-static stepped approach, in which the vessel was held in its mean dynamic floating position.

2.1 Benchmark LNG

For the benchmark study, MARIN's tank tests with a 135,000 m³ LNG Carrier [3] were replicated in CFD. During these tests, the model was towed at a constant speed whilst fixed to the carriage, prohibiting the model to freely sink and trim. In the CFD calculations, the tank walls and bottom were explicitly modelled to account for the tank blockage effect. The tank dimensions were obtained from the MARIN website.

OCIMF's past experience with obtaining member supplied hull models demonstrated difficulties related to confidentiality issues with the shipyards. Due to this experience compounded with the short time frame

available, the decision was made to use an alternative hull form available to LR for the modelling. Although the principal dimensions were similar, the design of the LR model dated back to the 1970's, resulting in a considerably different hull shape. The vessel was fitted with standard bilge keels stretching 30% of the length of the hull, and a NACA0016 rudder based on the GA. The propeller was omitted from the CFD calculations. The vessel scale factor was chosen such that the tank blockage, calculated as the ratio of model length between perpendiculars and tank width, was identical to the MARIN experiments.

Benchmarking was done against MARIN's CFD and experimental results for Wd/T ratios of 1.36 and 2.73 and current angles of 0, 45, 90, 135, and 180 degrees. This provided insight in the comparability of LR's CFD throughout the spectrum of cases considered.

2.2 Full curve development

The previous study, [2], indicated that ballast and laden draught coefficients were close to identical, arguably negating the need for separate curves. Therefore, the full curves were developed using the 150kDWT Post Marpol tanker from [2] at laden draught. Wd/T ratios were set to 1.02, 1.05, 1.10 and 3.00. In addition, one case was run with Wd/T 6.0 for a 60 degrees current angle. The current angles used for this revised report were 0, 10, 30, 60, 90, 120, 150, 170 and 180 degrees, with 0 degrees being stern on current. To verify that ballast and laden curves indeed remain similar if free sink and trim is taken into account, ballast cases were run for the afore mentioned Wd/T ratios at 60 degrees angle of current incidence.

For all cases, the flow domain extended to more than 4 ship lengths upstream, 4 ship lengths to port and starboard and over 6 ship lengths downstream. The current velocity was prescribed at the inlet, port and starboard boundaries, using the 1/7 power law with a flow speed of 2.06 m/s at the free surface. The layout of the computational domain is provided in **Figure 1**.

To study the effects of vessel size and shape, simulations were also performed with 50kDWT and 300kDWT tankers, using a 60 and 150 degrees of current incidence and Wd/T ratios 1.02 and 1.10. The 50kDWT vessel was about 180 metres in length, with a beam of 32.2 metres and a scantling draught of 12.5 metres. The hull was fitted with standard bilge keels stretching 30% of the vessels length and a NACA0016 rudder, based on the GA profile. Similarly, the 300kDWT tanker was about 330 metres in length, with a beam of 60 metres, a scantling draught of 22.6 metres and was also fitted with 30%L standard bilge keels and a NACA0016 rudder. For neither of the vessels the propeller was taken into account.

2.3 LNG carrier

The applicability of the current curves to LNG vessels was studied by comparing like for like CFD simulations for current angles of 30 and 60 degrees and water depth to draught ratios of 1.10 and 3.0. The LNG carrier used in this part was the full scale equivalent of the one used in the benchmarking exercise. Given that her length between perpendiculars was similar to that of the 150kDWT tanker, identical grid settings and domain dimensions could be used. The main differentiator between the LNG and tanker hull forms is, of course, the much lower block coefficient of the LNG carrier, resulting in much sharper bow and stern lines, compared to the much rounder tanker hull form.

2.4 Current sensitivity

OCIMF's current coefficients [1] are generated by making the current forces dimensionless, by dividing them by the product of 0.5, the water density, the vessel's length (*squared for the yaw-moment coefficient*), the draught and the current velocity squared. This implicitly assumes that there is a quadratic

relation between force and speed, over the range of current speeds typically encountered by moored vessels.

To investigate the coefficients' sensitivity to an increase in the current speed, 6 conditions were run with the 50kDWT tanker in which the current speed was increased to 3.09 m/s from 2.06 m/s. Water depth to draught ratios were set to 1.02, 1.05 and 1.10 and the flow angles to 30 and 60 degrees.

3. Results

3.1 Benchmark LNG

It should be noted that for the Benchmark LNG study, calculations were carried out at model scale, with the vessel fixed in space and that the tanks walls and bottom were explicitly modelled in the CFD simulation.

A mesh sensitivity study was carried out using 5 different mesh sizes, a current angle of 90 degrees and Wd/T ratio of 1.36. The results, reported in **Figure 2**, indicate that all results are within 1% for all meshes, with a negligible difference between the three finest meshes. The "Fine" mesh setting was used for the results reported below.

In general, the LR results compare very well with both MARIN's experimental and CFD results for Wd/T 1.36 and Wd/T 2.73, plotted in **Figure 3** and **Figure 4** respectively. It is duly noted that the C_x forces are relatively small and would therefore be sensitive to, for example, vibrations on the towing carriage and geometrical details.

LR's C_y value for 90 degrees is slightly higher on deep water, Wd/T 2.73, and slightly lower on shallow water, Wd/T 1.36, compared to both sets of MARIN results. To investigate the influence of hull geometry, two additional CFD calculations were performed at 90 degrees and Wd/T 1.36. For these calculations, the 150kDWT tanker (Pre-Marpol) and the Duisburg Test Case (DTC, large container ship) hull forms were scaled to have identical blockage to the LNG Carrier towing tank tests. The results, plotted in **Figure 4**, indicate that some variation in the results should be expected due to differences in hull geometries.

3.2 Full curve development

Similar to the Benchmark study, a mesh sensitivity study was carried out for the full curve development, using a 90 degrees angle of current incidence, Wd/T ratio of 1.10 and 5 different mesh sizes. For C_y, the results of all 5 meshes are within 3% from each other, as plotted in **Figure 5**. In the interest of time, the calculations in the remainder of this report were carried out using a mesh size in-between the medium and fine mesh, for it offered the best compromise between accuracy and required computation time.

The results for the lowest under keel clearance, Wd/T 1.02, are presented in **Table 1** and **Figure 6**. It is duly noted that no curves were published in [1] for this condition. Therefore, for comparison purposes, the closest available OCIMF curves are plotted with green lines and triangles. The CFD curves indicate that at this low Wd/T ratio there is a noticeable effect of FST and that this effect is stronger for ballast draught. The non-zero, but small, transverse forces and moments in head-on and stern-on current are due to the asymmetry in the flow induced by the propeller.

For the slightly higher Wd/T ratio of 1.05, the contribution of free sink and trim is reducing, as shown in **Table 2** and **Figure 7**. Notably, the overall shape of the curves is consistent with the results found for Wd/T 1.02, with the main differences found around 150 degrees of current incidence. Thereby, the difference between ballast and laden draught results is reduced as well.

A good correlation is shown in **Table 3** and **Figure 8** for Wd/T 1.10 between the published OCIMF curves and the CFD calculations. The main difference in C_y , between current angles of 60 and 120 degrees, is most probably the result of tank blockage effects present in the OCIMF curves. These will be discussed in more detail in Section 4. In line with the trend, the difference between laden and ballast draught conditions has further reduced.

For the highest under keel clearance of Wd/T 3.0, there is a very good agreement between the published OCIMF curves and LR's CFD calculations, as presented in **Table 4** and **Figure 9**. These results underline Marin's observation in [3] that tank blockage effects would not have played a significant role during these tests. In addition to the Wd/T 3.0 curves, the calculation results of the 60 degrees, Wd/T 6.0 calculations have also been added to the plot. In line with OCIMF's publication [1], these results show a diminishing impact of under keel clearance on the current loads.

To showcase the influence of vessel size on the force coefficients, calculations were carried out with 50kDWT and 300kDWT tankers at water depth to draught, Wd/T , ratios of 1.02 and 1.10 and current angles of 60 and 150 degrees. The results, respectively tabulated in **Table 5** and **Table 6**, plotted in **Figure 10** and **Figure 11**, suggest that the influence of vessel size and shape on the force coefficients is marginal, with the notion that the differences observed around 150 degrees are likely caused by hydrodynamic lift.

3.3 LNG carrier

Given that the full scale LNG carrier was of similar length as the 150kDWT Post Marpol tanker, used to develop the full curves, identical numerical grid settings were used. The force coefficients for the conditions considered, 30 and 60 degrees on Wd/T 1.10 and 3.0 are plotted in **Figure 12** and **Figure 13** respectively. All numerical results are summarised in **Table 7**.

The results indicate that one can expect slightly smaller axial forces and moments and a slightly higher transverse force, relative to a tanker of similar length and draught. This is likely to be due to the sharper bow form of the LNG carrier, resulting in a slightly larger and stronger vortex being shed.

3.4 Current sensitivity

To study the sensitivity of the current coefficients to the current velocity, the speed was increased from 2.06 to 3.09 m/s. All cases were run with the 50kDWT tanker, using current angles of 30 and 60 degrees and water depth to draught ratios of 1.02, 1.05 and 1.10. The results are respectively plotted in **Figure 14**, **Figure 15** and **Figure 16**.

By comparing the numerical results in **Table 8**, with those in **Table 5**, one observes only marginal differences, leading to the conclusion that the same coefficients can indeed be used for current velocities of 2.06m/s and 3.09m/s. The differences are mainly caused by a slight increase in sinkage and trim, due to the higher velocities below the flat of bottom.

4. Discussion

4.1 Benchmark LNG

The towing tank tests conducted and reported by MARIN in [3] had a rather unique setup, in that the vessel was restricted in all degrees of freedom. This allows for a one-to-one replication of the towing tank setup in CFD, provided that all data is available. In numerous previous studies, good agreement has been found between CFD and experimental results, to which the results in [3] are no exception.

There are, however, a few factors that are likely to have contributed to the observed differences between LR's CFD calculations and those from MARIN. Most notably, there will be geometric differences in the hull lines, bilge keels, propeller (*included in the experiments*) and rudder; the latter two will generate hydrodynamic lift under the right inflow angles.

Arguably, the biggest differences will have been caused by the bulbous bow. Where MARIN's LNG carrier represented a modern design, the hull geometry used by LR dated back to the 1970's and had more of a s-shaped bow, rather than a bulbous bow. Especially important is the riding height of the bulbous bow, with respect to the free surface. Given its short width, the bulbous bow would have generated some free surface deformation.

It is further noted that the calculated tank blockage was based on the towing tank width and the vessel's length between perpendiculars, rather than the project areas of tank and vessel. This was mainly due to the projected, or lateral underwater, area not being provided in [3]. Based on the findings in [3], this would mostly influence current angles between 60 and 120 degrees.

The combined effect of these factors is the most likely reason behind the small differences observed in calculated coefficients between LR and MARIN CFD.

4.2 Full curve development

The decrease in water depth to draught ratio results in a transition of the flow pattern surrounding the vessel. For deep water, $Wd/T \geq 3.0$, the flow has a three dimensional behaviour, with a large portion of the flow passing underneath the flat of bottom, as pictured in **Figure 17**. This figure, as well as the next three, is a snapshot in time for the flow pattern around the 150kDWT Post Marpol tanker, at a 60 degree angle of current incidence in its fixed position. The streamlines originate from a line 200 metres upstream of the vessel that is perpendicular to the keel line. The velocity plane is also situated in the same plane as the flat of bottom. In the next three figures only the water depth to draught ratio is changed.

When the Wd/T ratio reduces to 1.10, substantially less water passes underneath the vessel and we observe flow accelerations around the bow and stern, shown in **Figure 18**. The velocity field aft of the vessel also indicates that larger scale vortices are being shed.

The strength of the vortical structures develops further when the Wd/T ratio reduces to 1.05. A clear shedding pattern emerges in **Figure 19** and the streamlines remain longer in-plane. This indicates that the flow is transitioning to two dimensional behaviour.

On the lowest water depth to draught ratio, depicted in **Figure 20**, very few streamlines changing depth and the strength (*rotational speed*) of the vortical structures has increased. If one would reduce to Wd/T ratio to its minimum value of 1.0, the emerging flow pattern will likely show even stronger vortices being generated and a flatter streamline pattern with respect to the vertical (*out-of-plane*) direction.

The coefficients will therefore theoretically converge to the values for Wd/T 1.0. However, it is arguable whether the vessel can dynamically ever reach that position, for a repulsive vertical force will likely be generated, not dissimilar to bank effects in rivers.

The dynamic sink and trim, resulting from a dynamic low pressure region underneath the hull, effectively reduces Wd/T ratio. This is shown in **Figure 21**, where the blue line represents the C_y coefficients at 90 degrees of current incidence with the vessel in its “fixed” position. The red line provides the results for the FST calculations plotted against the initial Wd/T ratio. The green line plots the same FST results against the dynamic Wd/T ratio, only taking into account sinkage. Based on this figure it can be concluded that, by close approximation, the “dynamic” current coefficients can be found using the “fixed” coefficient curves and the “dynamic” Wd/T ratio.

In a similar way, dynamic sink and trim will contribute to the model tank based coefficients being slightly higher. Due to the thicker boundary layer underneath the hull, the maximum flow velocity between hull and tank bottom will be relatively higher, leading to a larger trim and sinkage. This might be counteracted, in part, by how the too low Reynolds numbers will influence the formation and dissipation of the vortical structures, for the tank tests do not obey Reynolds scaling. It is duly noted that the tank blockage effects, on the other hand, are driven by pressure build-up inside a “restricted” waterway.

The distinct peak in C_x coefficient observed at 150 degrees angle of current incidence, **Figure 7** and **Figure 8**, can most likely be attributed to the generation of hydrodynamic lift, where the bow is considered to be the leading edge of the profile. The fullness of the bow will determine where and when flow will separate, making this part of the curves sensitive to variations in shape. This becomes apparent in **Figure 11**, where the C_x values for the 50kDWT and 300kDWT tankers vary substantially.

At ballast draught, it is not just the dynamic floating position of the vessel that will influence the current coefficients, as shown by direct comparison in **Figure 22**. The increase in C_y for identical Wd/T values higher than 3.0, is a direct result of the stronger vortical structures being generated. For the Wd/T 3.0 condition, one observes little difference between the ballast draught, **Figure 23**, and laden draught, **Figure 17** streamlines. On Wd/T 1.10, the ballast draught shows already clearly defined vortices in **Figure 24**, where on the laden draught they are just starting to form, see **Figure 18**.

For the even lower Wd/T ratios of 1.05 and 1.02, plotted in **Figure 25** and **Figure 26**, it is obvious that a strong 2D flow regime is established, with virtually no water passing underneath the keel. This raises the question whether or not the ballast and laden draught coefficients would converge to the same value for Wd/T 1.0, or that they will be different due to the more cylindrical cross section of the hull form on ballast draught.

The comparison with the 50kDWT and 300kDWT tankers indicated only a marginal change in the current coefficients. The streamlines on Wd/T 1.10 and 60 degrees, plotted in **Figure 27** and **Figure 28**, are therefore rather similar as those seen in **Figure 18**. Arguably, however, there could be some influence of the water depth, but the differences are too small to state this for certain.

4.3 LNG Carrier

Based on the discussion above, one can deduct that the lateral forces for the LNG carrier must be higher compared to her 150kDWT Post Marpol tanker counterpart, by simply comparing the streamline plots in **Figure 29** and **Figure 18**. The sharper bow and stern of the LNG vessel results in a larger pressure gradient aft of the flow separation point, resulting in a stronger vortex being shed and hence a larger lateral force coefficient.

4.4 Current sensitivity

The higher flow velocity logically leads to an increase in sink and trim, an effect that becomes stronger the further the current becomes beam on. As a result, small changes in the flow pattern, plotted in **Figure 30**, can be seen other than the obvious increase in speed.

5. Conclusions

Based on the results and discussion, the following conclusions can be drawn:

- LR CFD results compare well with equivalent calculations conducted by MARIN in [3].
- Current coefficients for free sink and trim can be closely approximated by applying the dynamic Wd/T ratio, which takes into account sinkage, to the curves derived from fixed CFD calculations
- The current coefficients show a marginal sensitivity to vessel size and shape, with the sharper form resulting generally in larger forces.
- The CFD derived current curves could be applied for LNG Carriers if an additional safety margin is taken into account for the lower Wd/T ratios.
- The current coefficients are only marginally sensitive to the current speed, due to relative changes in the dynamic floating position. This sensitivity is in the same order as the sensitivity to hull shape, which can be up to 10%.

6. Recommendations

The following recommendations are made:

- Calculate the force coefficients at Wd/T 1.00 on both laden and ballast draught to verify they converge to the same values.
- Calculate the force coefficients at Wd/T 1.50 on laden draught to allow for a smoother transition between the CFD derived curves at the same angle of current incidence.

7. References

- [1] OCIMF – *Prediction of Wind and Current Loads on VLCCs* – Second Edition – 1994 – ISBN 13: 978 1 85609 042 1 & ISBN: 10: 1 85609 042 6
- [2] LR EMEA, TID – *Current drag comparison including free sink and trim for Pre- and Post Marpol tankers* – TID7796C-Revision1 – September 2016
- [3] A. Koop – *Shallow water current loads on a LNG carrier using CFD* – OMAE2015-41275 – June 2015.

Tables

Table 1: Full curve development – Results Wd/T 1.02	12
Table 2: Full curve development – Results Wd/T 1.05	12
Table 3: Full curve development – Results Wd/T 1.10	13
Table 4: Full curve development – Results Wd/T 3.00 and Wd/T 6.00 (Deep)	13
Table 5: Full curve development – Results 50kDWT	14
Table 6: Full curve development – Results 300kDWT	14
Table 7: LNG carrier – Results	14
Table 8: Current sensitivity – Results	14

Angle	Cx – Fixed	Cy – Fixed	Cxy – Fixed	Cx – FST	Cy – FST	Cxy - FST
0	0.072	0.111	-0.002	0.071	0.105	-0.003
10	0.008	0.503	-0.190	0.015	0.471	-0.185
30	0.197	0.757	-0.238	0.200	0.837	-0.235
60	0.248	2.107	-0.195	0.288	2.405	-0.187
90	0.095	2.729	-0.016	0.091	2.914	-0.037
120	-0.134	2.287	0.126	-0.146	2.832	0.098
150	-0.146	0.908	0.188	-0.136	0.938	0.195
170	0.043	0.611	0.204	0.027	0.512	0.203
180	-0.056	0.141	0.000	-0.055	0.145	-0.001
Ballast	0.299	2.528	-0.127	0.302	3.223	-0.089

Table 1: Full curve development – Results Wd/T 1.02

Angle	Cx – Fixed	Cy – Fixed	Cxy – Fixed	Cx – FST	Cy – FST	Cxy - FST
0	0.042	0.005	0.000	0.043	0.006	0.000
10	0.005	0.404	-0.173	0.005	0.435	-0.175
30	0.160	0.629	-0.242	0.164	0.645	-0.239
60	0.228	1.899	-0.196	0.246	1.983	-0.182
90	0.076	2.249	-0.028	0.086	2.584	-0.012
120	-0.086	1.745	0.136	-0.104	2.055	0.137
150	0.320	1.540	0.357	-0.103	0.963	0.197
170	0.037	0.675	0.165	0.042	0.681	0.177
180	-0.034	0.000	0.000	-0.034	0.000	0.000
Ballast	0.254	2.291	-0.127	0.317	2.532	-0.113

Table 2: Full curve development – Results Wd/T 1.05

Angle	Cx – Fixed	Cy – Fixed	Cxy – Fixed	Cx – FST	Cy – FST	Cxy - FST
0	0.034	0.009	-0.001	0.034	0.009	-0.001
10	0.014	0.318	-0.135	0.013	0.312	-0.140
30	0.084	0.660	-0.243	0.098	0.635	-0.238
60	0.152	1.377	-0.198	0.162	1.580	-0.205
90	0.046	1.855	-0.036	0.050	1.961	-0.033
120	-0.056	1.466	0.130	-0.070	1.660	0.134
150	0.355	1.538	0.335	0.353	1.573	0.360
170	0.004	0.523	0.117	-0.030	0.529	0.123
180	-0.023	0.004	0.001	-0.023	0.004	0.001
Ballast	0.156	1.666	-0.185	0.223	2.245	-0.135

Table 3: Full curve development – Results Wd/T 1.10

Angle	Cx – Fixed	Cy – Fixed	Cxy – Fixed	Cx – FST	Cy – FST	Cxy - FST
0	0.022	0.016	-0.005	0.022	0.015	-0.004
10	0.023	0.041	-0.033	0.023	0.041	-0.033
30	0.011	0.299	-0.074	0.011	0.300	-0.075
60	-0.015	0.886	-0.095	-0.013	0.894	-0.095
90	0.020	1.058	0.000	0.022	1.062	0.000
120	0.035	0.938	0.087	0.025	0.943	0.088
150	0.003	0.350	0.057	0.003	0.352	0.057
170	-0.015	0.064	0.027	-0.015	0.064	0.027
180	-0.014	0.000	0.000	-0.014	0.000	0.000
Ballast	0.021	0.649	-0.058	0.021	0.670	-0.062
Deep	-0.023	0.733	-0.077	-0.023	0.744	-0.077

Table 4: Full curve development – Results Wd/T 3.00 and Wd/T 6.00 (Deep)

Wd/T	Angle	Cx – Fixed	Cy – Fixed	Cxy – Fixed	Cx – FST	Cy – FST	Cxy - FST
1.02	60	0.254	2.315	-0.117	0.259	2.479	-0.124
1.02	150	-0.167	1.069	0.196	-0.144	1.034	0.215
1.10	60	0.100	1.421	-0.187	0.119	1.712	-0.195
1.10	150	0.037	1.034	0.238	-0.050	0.807	0.203

Table 5: Full curve development – Results 50kDWT

Wd/T	Angle	Cx – Fixed	Cy – Fixed	Cxy – Fixed	Cx – FST	Cy – FST	Cxy - FST
1.02	60	0.267	1.879	-0.220	0.286	1.919	-0.222
1.02	150	-0.136	0.969	0.181	-0.141	1.035	0.183
1.10	60	0.168	1.302	-0.207	0.174	1.395	-0.215
1.10	150	0.251	1.343	0.306	0.263	1.372	0.323

Table 6: Full curve development – Results 300kDWT

Wd/T	Angle	Cx – Fixed	Cy – Fixed	Cxy – Fixed	Cx – FST	Cy – FST	Cxy - FST
1.10	30	0.018	0.856	-0.184	-0.044	1.035	-0.205
1.10	60	0.051	1.613	-0.125	0.014	2.129	-0.079
3.00	30	0.007	0.285	-0.044	0.007	0.288	-0.044
3.00	60	0.003	0.873	-0.050	0.002	0.891	-0.052

Table 7: LNG carrier – Results

Wd/T	Angle	Cx – Fixed	Cy – Fixed	Cxy – Fixed	Cx – FST	Cy – FST	Cxy - FST
1.02	30	0.188	0.724	-0.229	0.190	0.855	-0.221
1.02	60	0.231	2.190	-0.159	0.221	2.500	-0.156
1.05	30	0.161	0.647	-0.229	0.173	0.662	-0.229
1.05	60	0.171	1.894	-0.181	0.234	2.258	-0.143
1.10	30	0.084	0.644	-0.223	0.124	0.606	-0.224
1.10	60	0.109	1.412	-0.180	0.157	1.881	-0.174

Table 8: Current sensitivity – Results

Figures

- Figure 1: Typical computational domain
- Figure 2: Benchmark LNG - Mesh sensitivity study
- Figure 3: Benchmark LNG – Wd/T 2.73 results
- Figure 4: Benchmark LNG – Wd/T 1.36 results
- Figure 5: Full curve development - Mesh sensitivity study results showing variation in Cy
- Figure 6: Full curve development - Wd/T 1.02 results
- Figure 7: Full curve development - Wd/T 1.05 results
- Figure 8: Full curve development - Wd/T 1.10 results
- Figure 9: Full curve development - Wd/T 3.0 results
- Figure 10: Full curve development - 50kDWT and 300kDWT results for Wd/T 1.02
- Figure 11: Full curve development - 50kDWT and 300kDWT results for Wd/T 1.10
- Figure 12: LNG carrier - Wd/T 1.10 results
- Figure 13: LNG carrier - Wd/T 3.0 results
- Figure 14: Current sensitivity - Wd/T 1.02 results
- Figure 15: Current sensitivity - Wd/T 1.05 results
- Figure 16: Current sensitivity - Wd/T 1.10 results
- Figure 17: Discussion – Streamlines, Laden, Wd/T 3.00, 60 degrees
- Figure 18: Discussion - Streamlines, Laden 17m, Wd/T 1.10, 60 degrees
- Figure 19: Discussion - Streamlines, Laden, Wd/T 1.05, 60 degrees
- Figure 20: Discussion - Streamlines, Laden, Wd/T 1.02, 60 degrees
- Figure 21: Discussion - Dynamic floating position, Laden, 90 degrees
- Figure 22: Discussion - Laden vs. Ballast comparison
- Figure 23: Discussion - Streamlines, Ballast, Wd/T 3.00, 60 degrees
- Figure 24: Discussion - Streamlines, Ballast, Wd/T 1.10, 60 degrees
- Figure 25: Discussion - Streamlines, Ballast, Wd/T 1.05, 60 degrees
- Figure 26: Discussion - Streamlines, Ballast, Wd/T 1.02, 60 degrees
- Figure 27: Discussion - 50kDWT, Laden 12.5m, Wd/T 1.10, 60 degrees, Streamlines
- Figure 28: Discussion - 300kDWT, Laden 22.6m, Wd/T 1.10, 60 degrees, Streamlines
- Figure 29: Discussion - LNG, Laden 11.8m, Wd/T 1.10, 60 degrees, Streamlines
- Figure 30: Discussion - 50kDWT, 3.09m/s, Laden 12.5m, Wd/T 1.10, 60 degrees, Streamlines

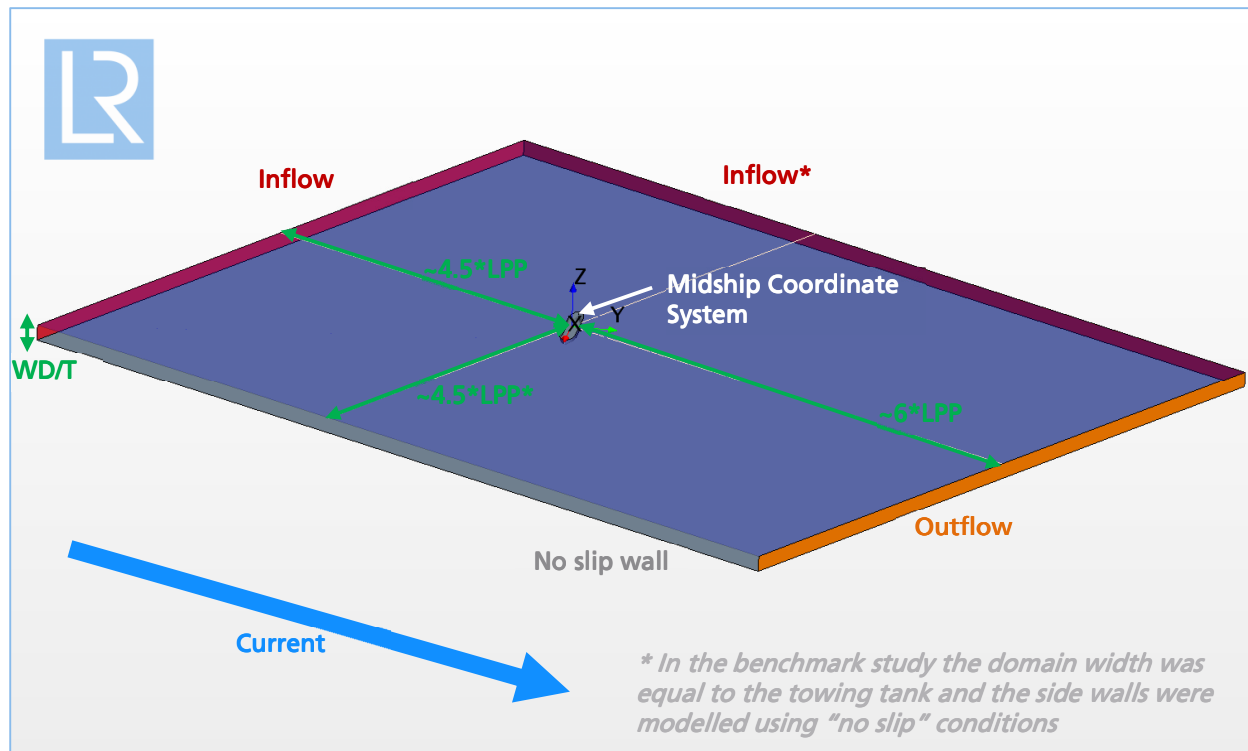


Figure 1: Typical computational domain

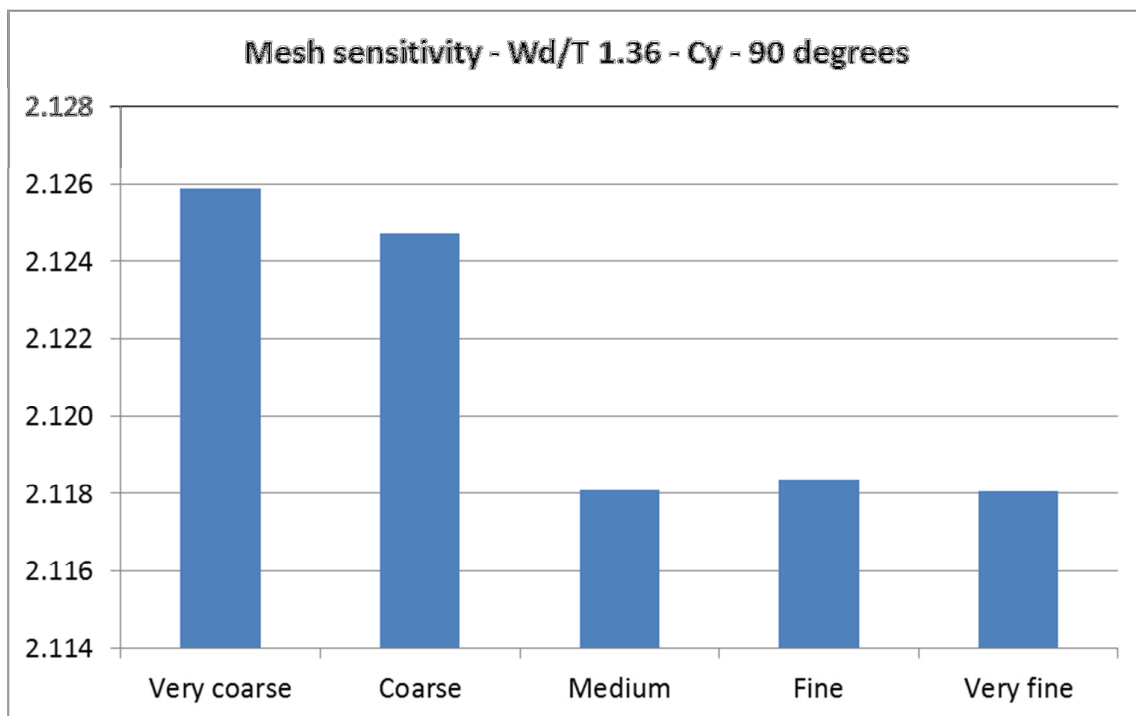


Figure 2: Benchmark LNG - Mesh sensitivity study

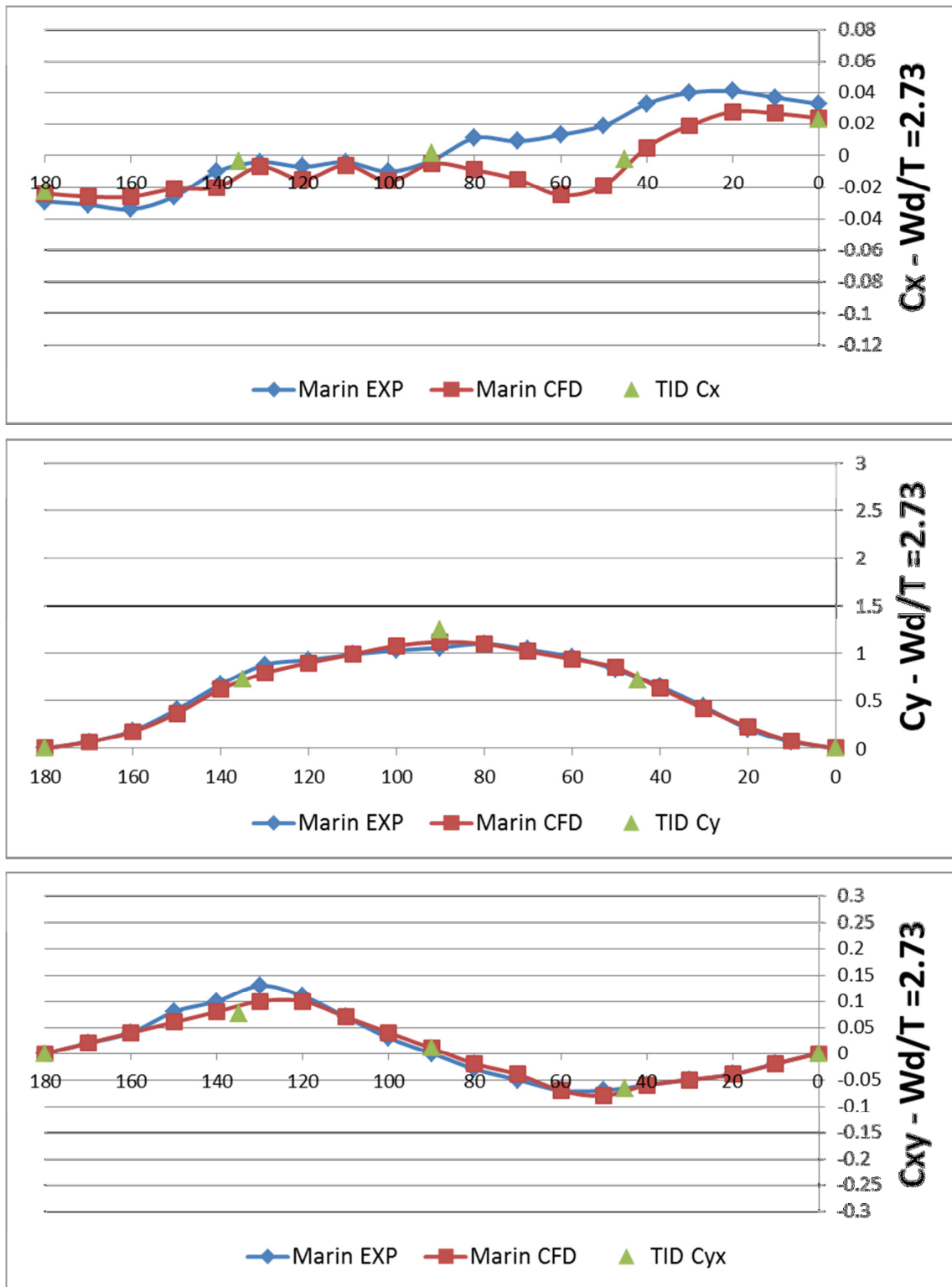


Figure 3: Benchmark LNG – Wd/T 2.73 results

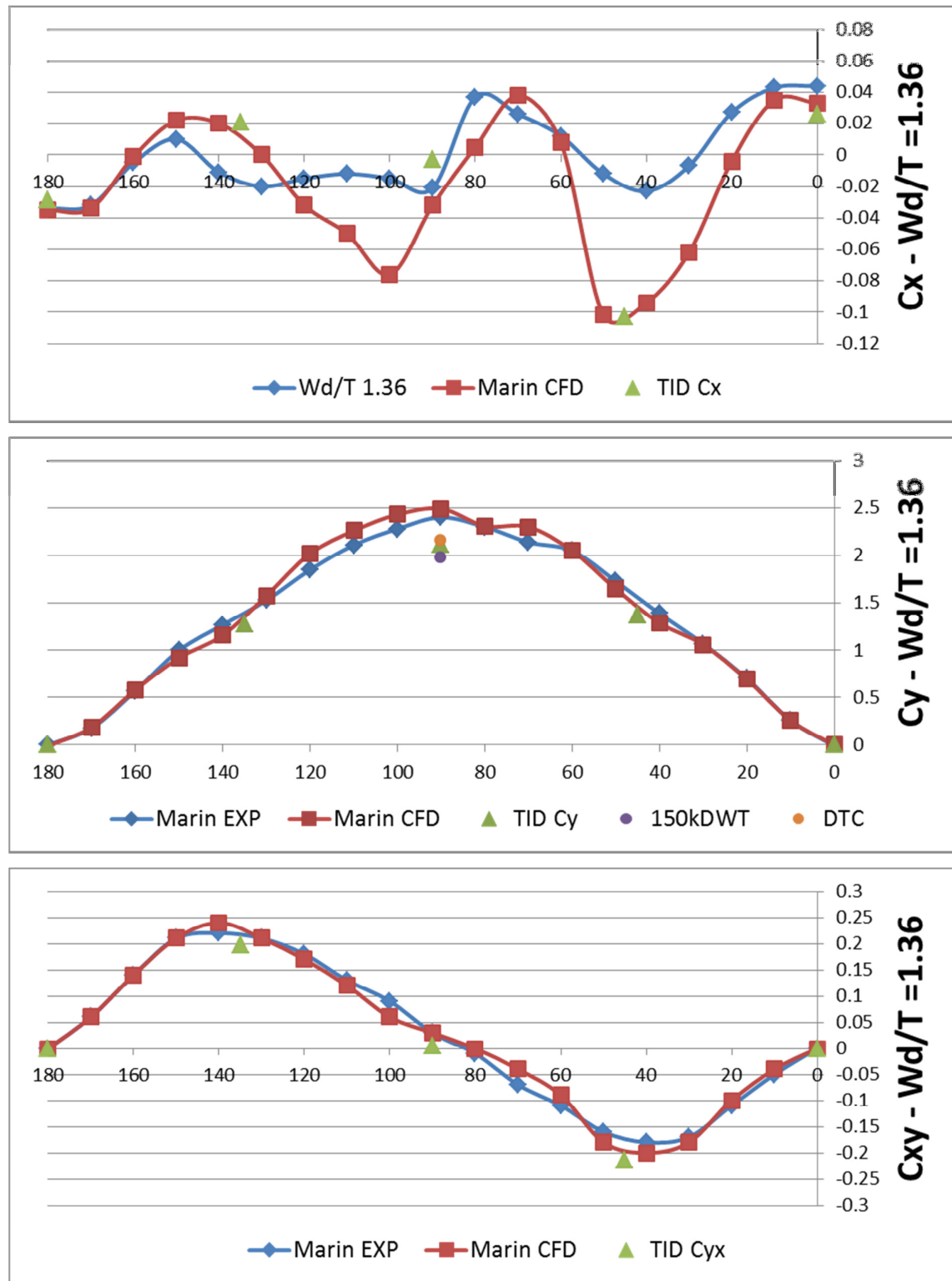


Figure 4: Benchmark LNG – Wd/T 1.36 results

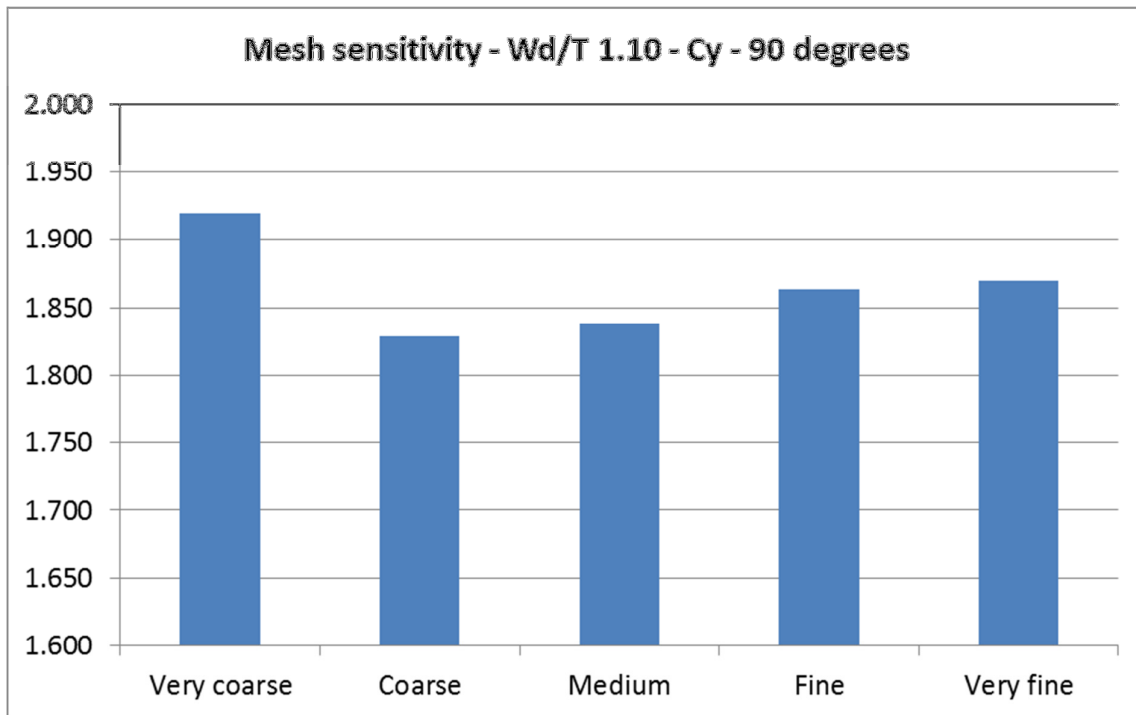


Figure 5: Full curve development - Mesh sensitivity study results showing variation in C_y

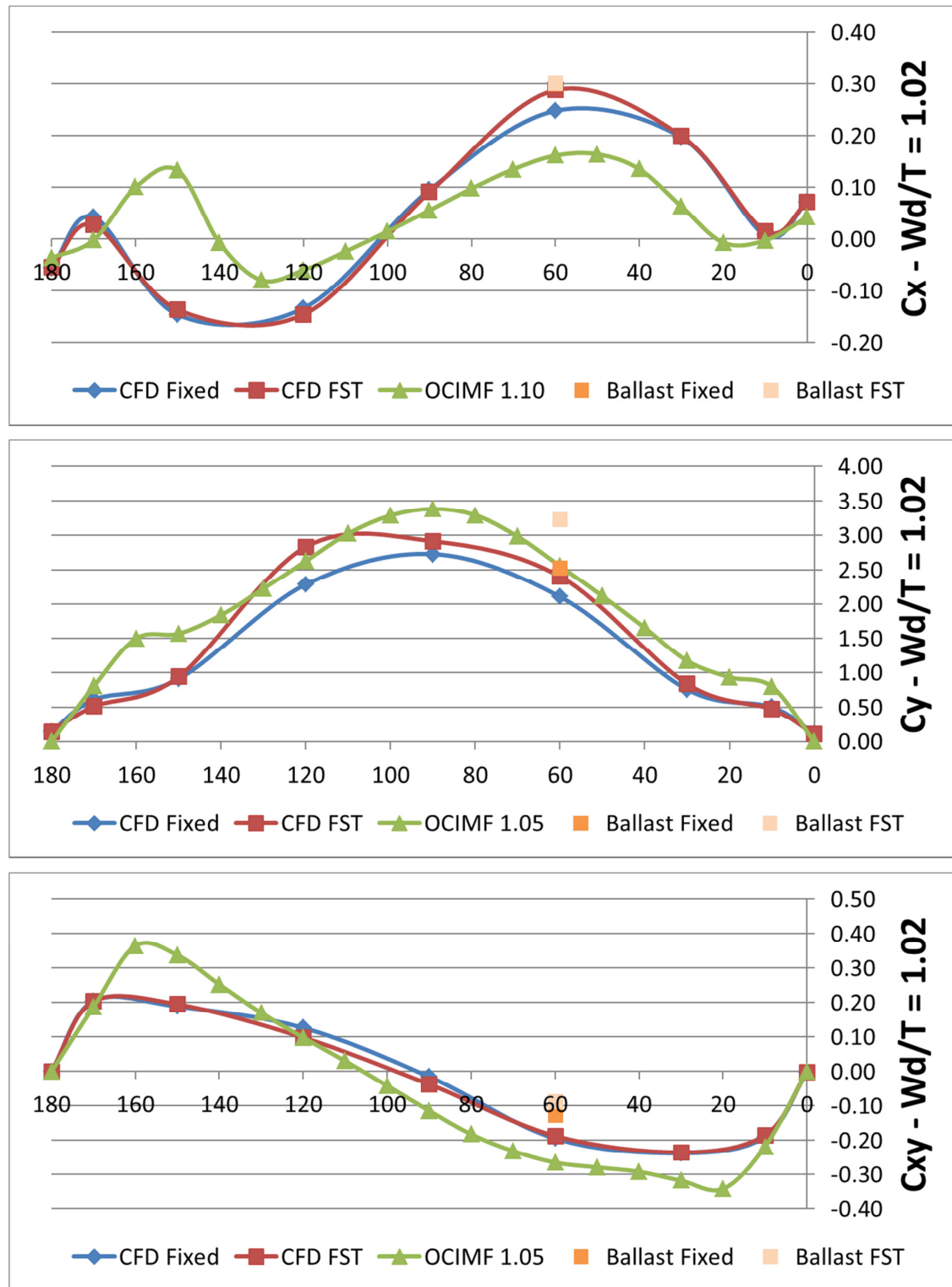


Figure 6: Full curve development - Wd/T 1.02 results

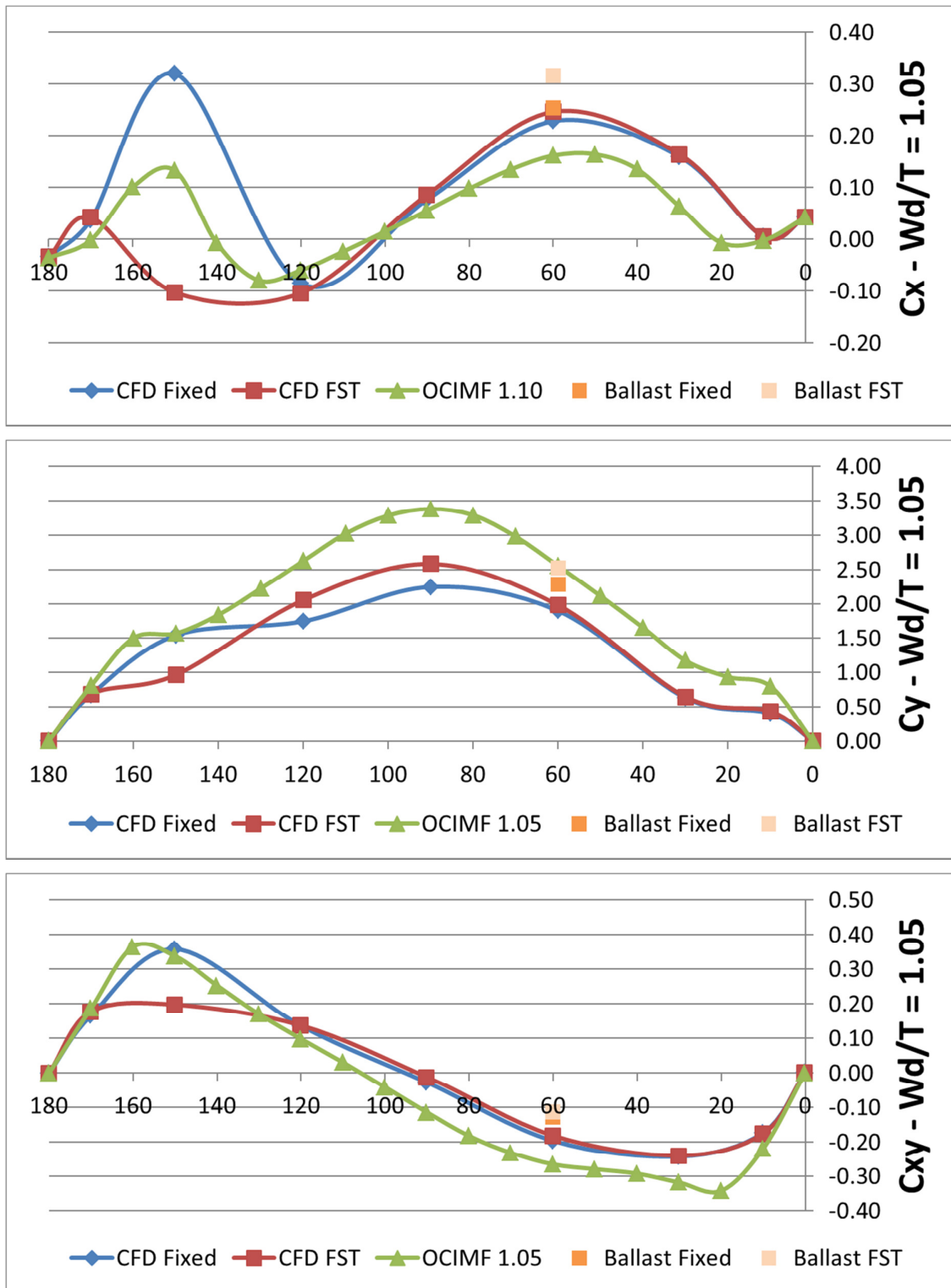


Figure 7: Full curve development - Wd/T 1.05 results

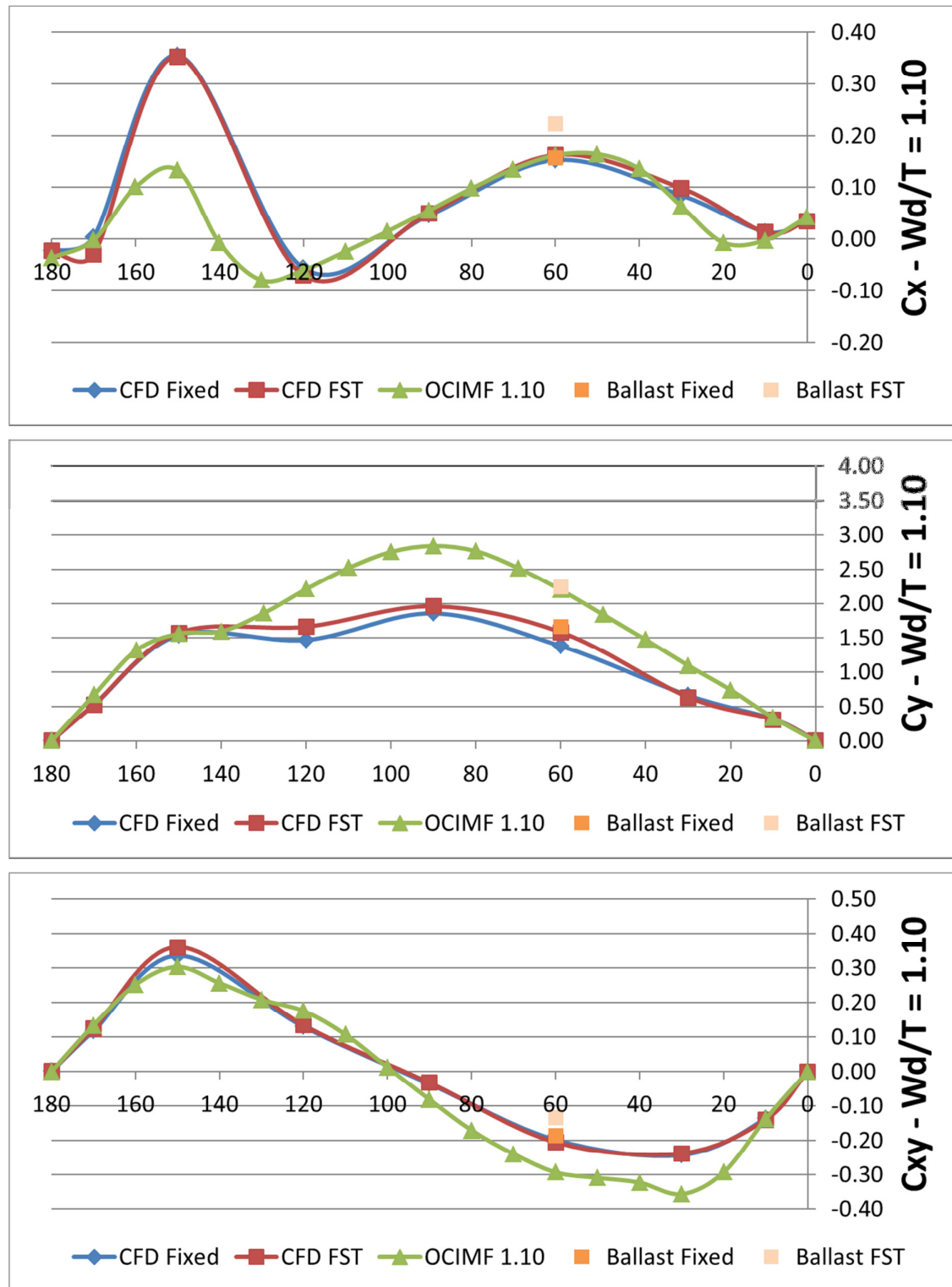


Figure 8: Full curve development - Wd/T 1.10 results

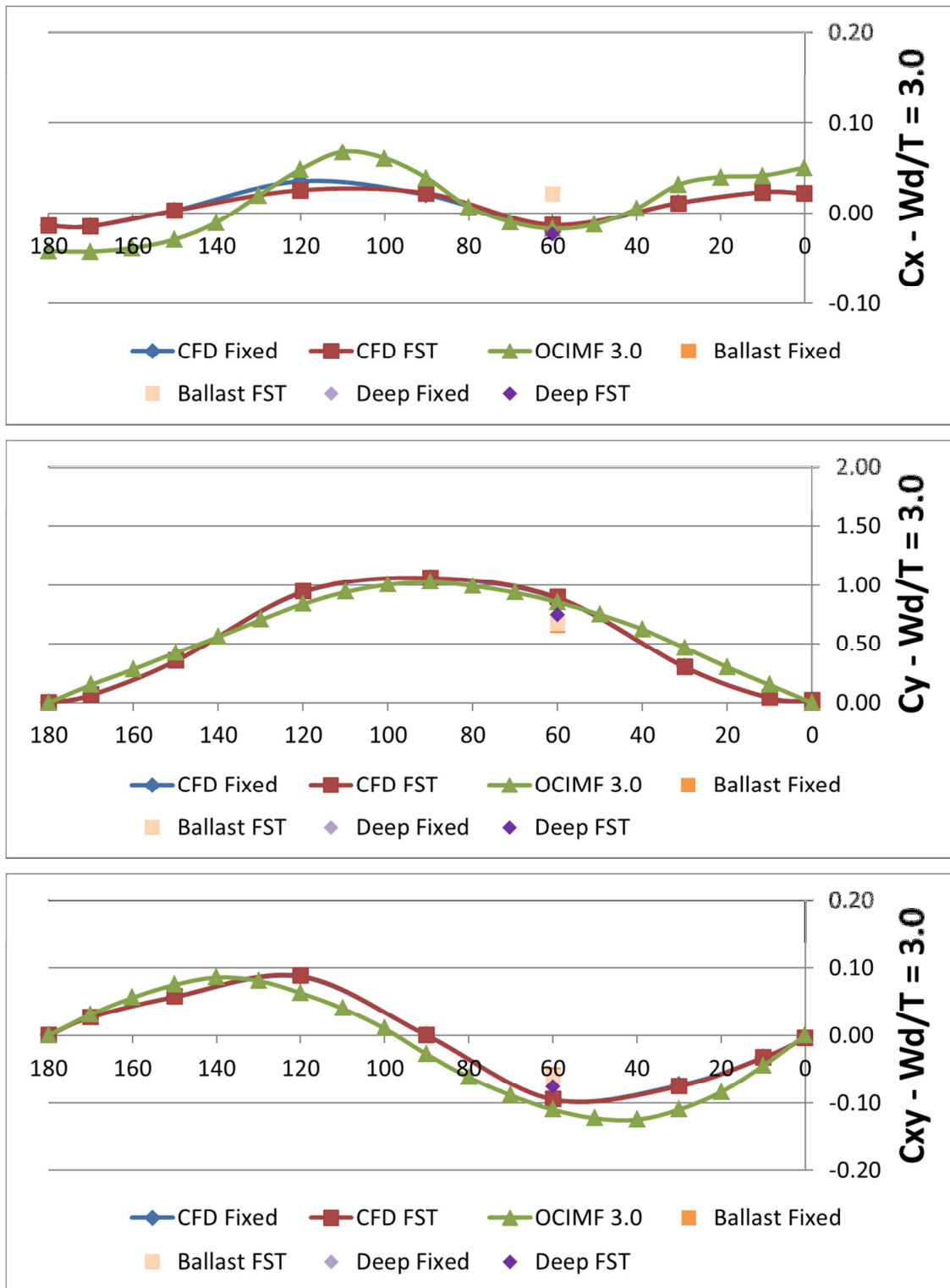


Figure 9: Full curve development - Wd/T 3.0 results

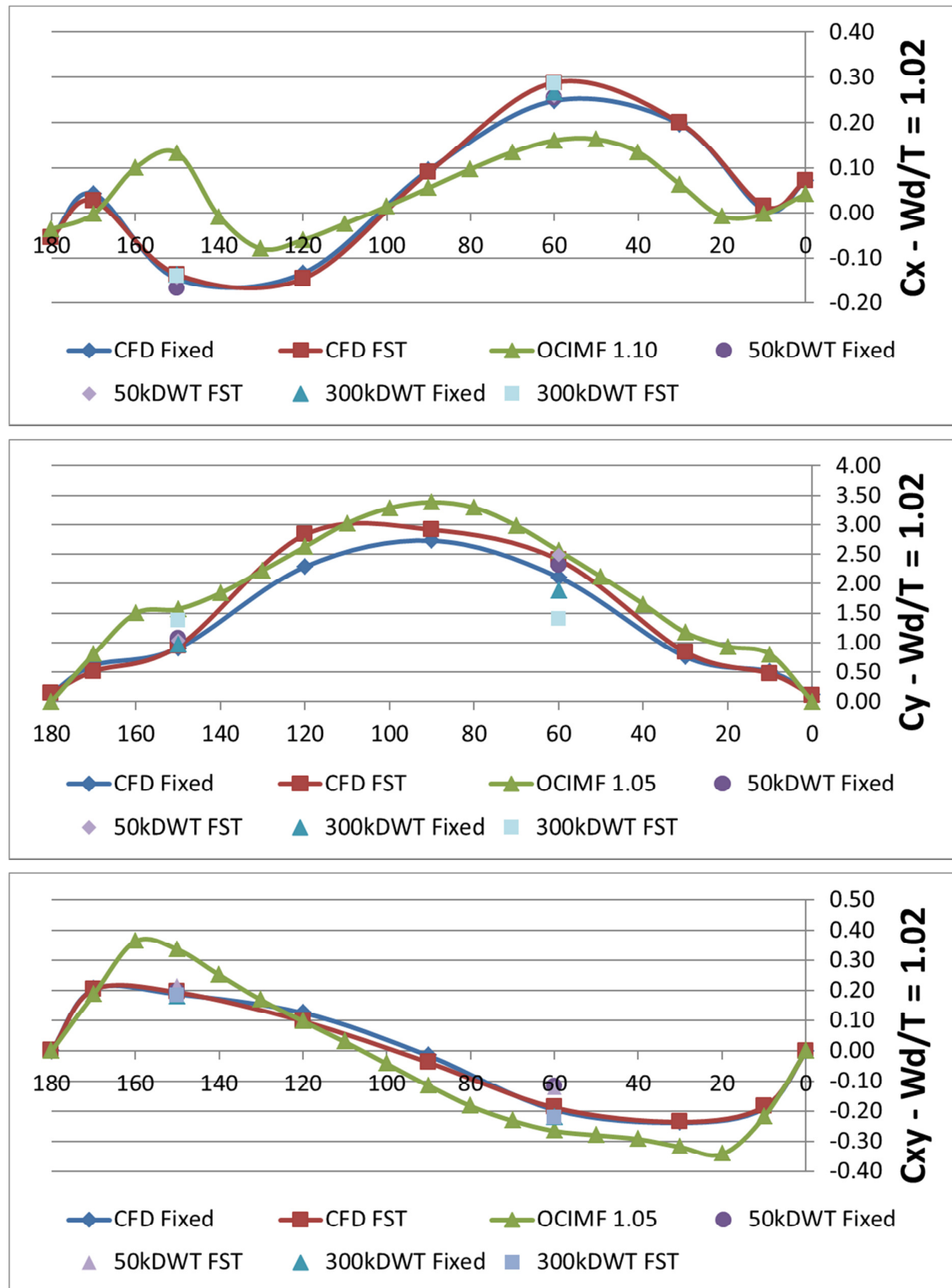


Figure 10: Full curve development - 50kDWT and 300kDWT results for Wd/T 1.02

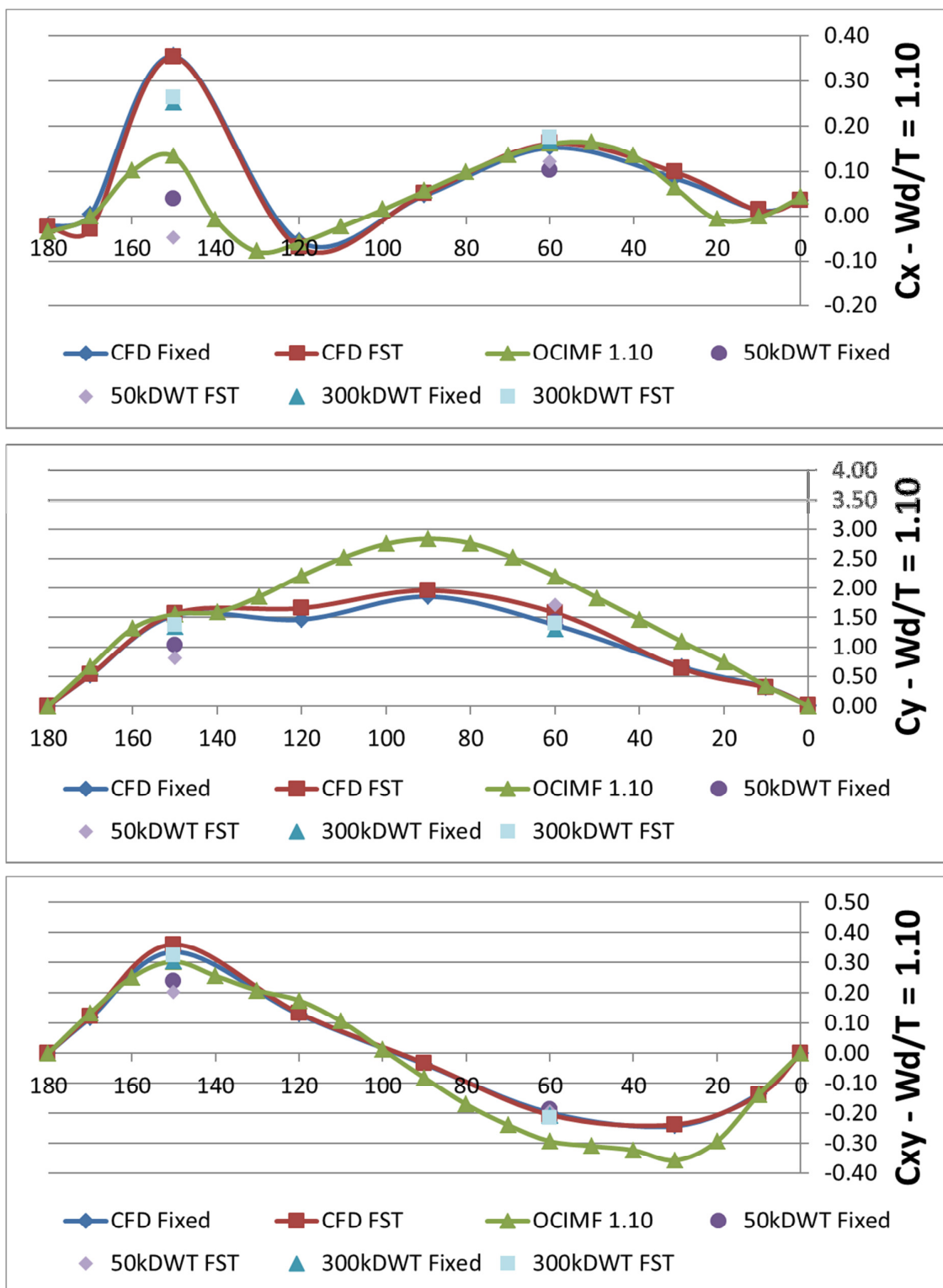


Figure 11: Full curve development - 50kDWT and 300kDWT results for Wd/T 1.10

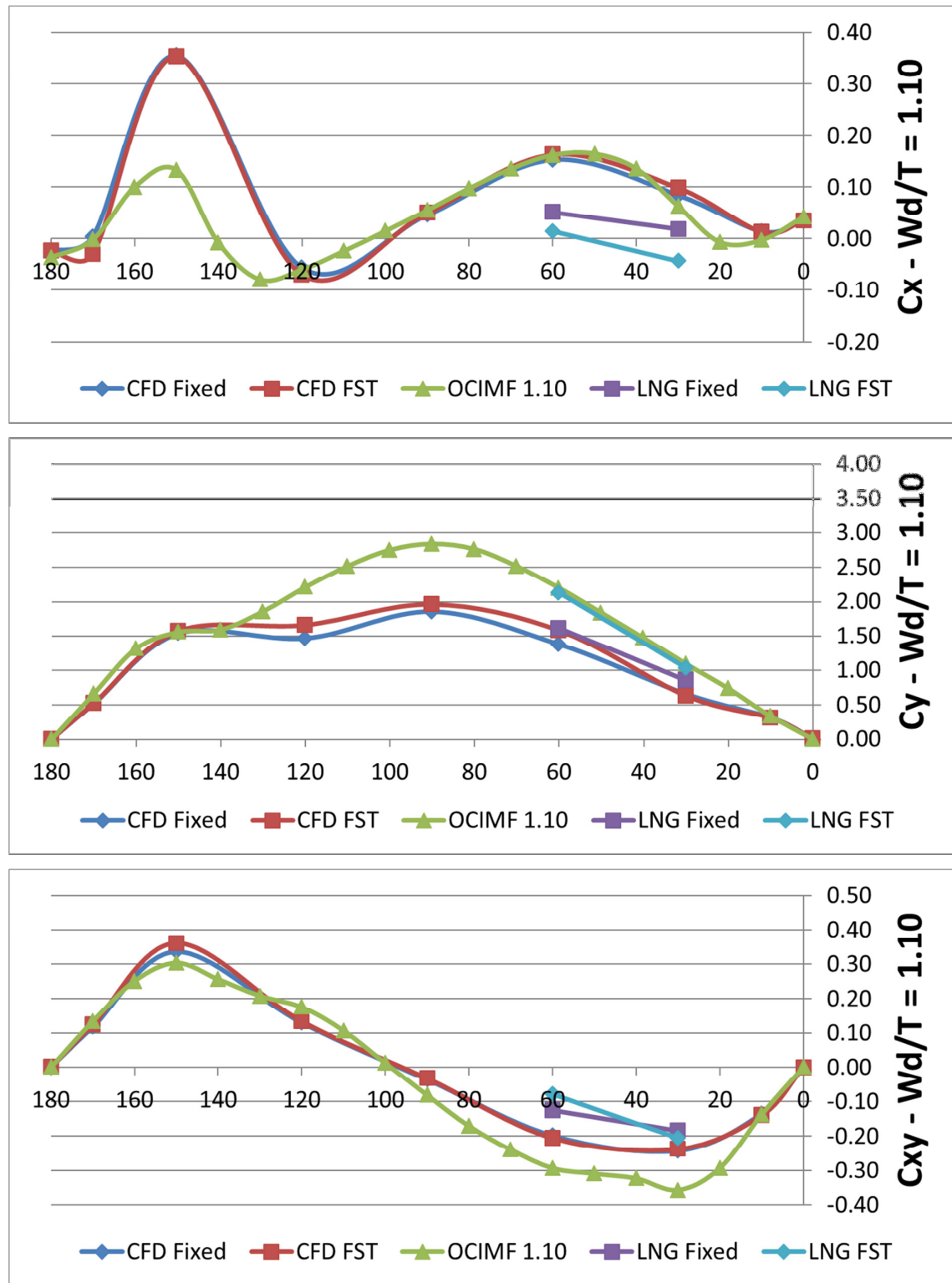


Figure 12: LNG carrier - W_d/T 1.10 results

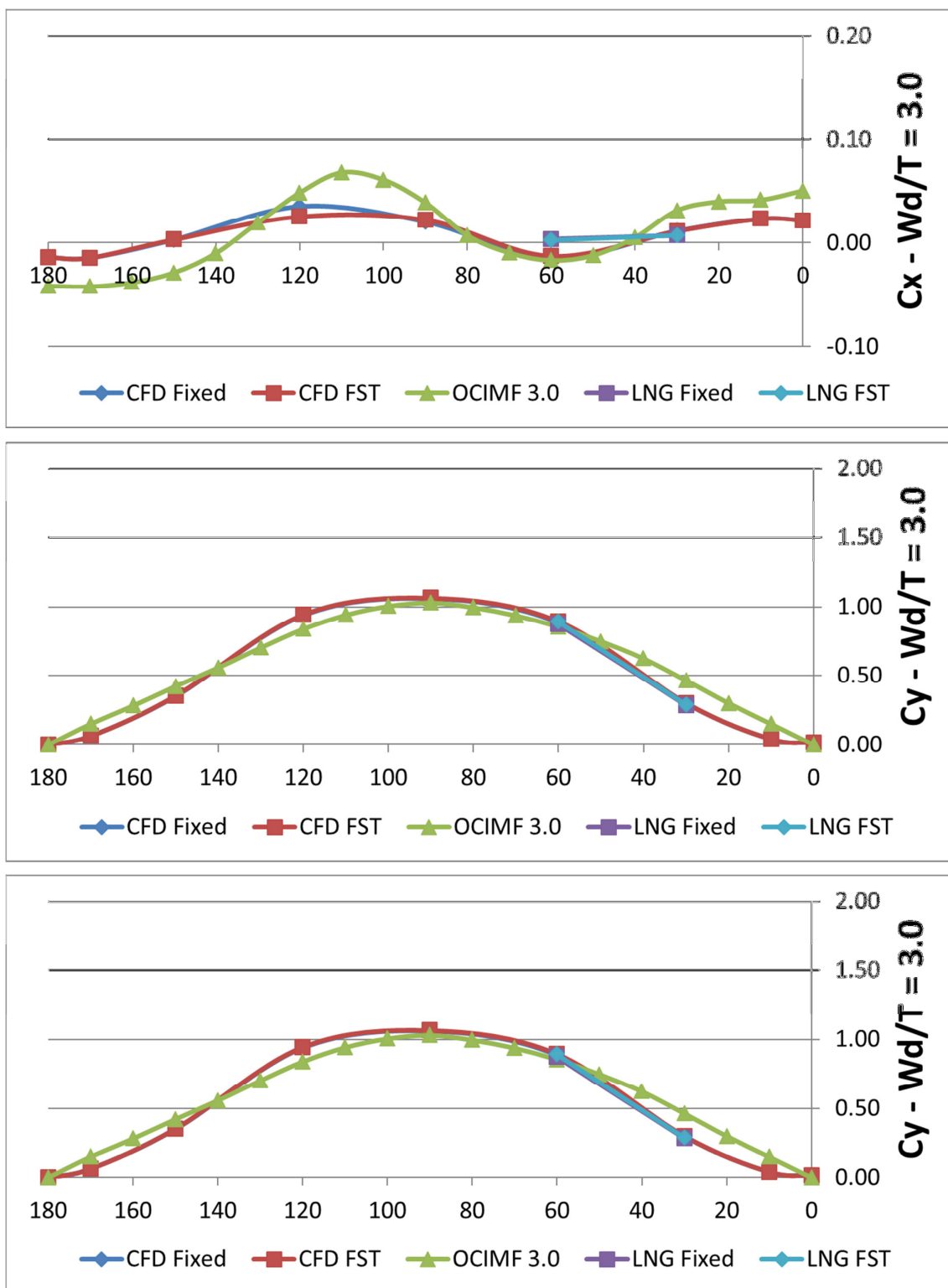


Figure 13: LNG carrier - Wd/T 3.0 results

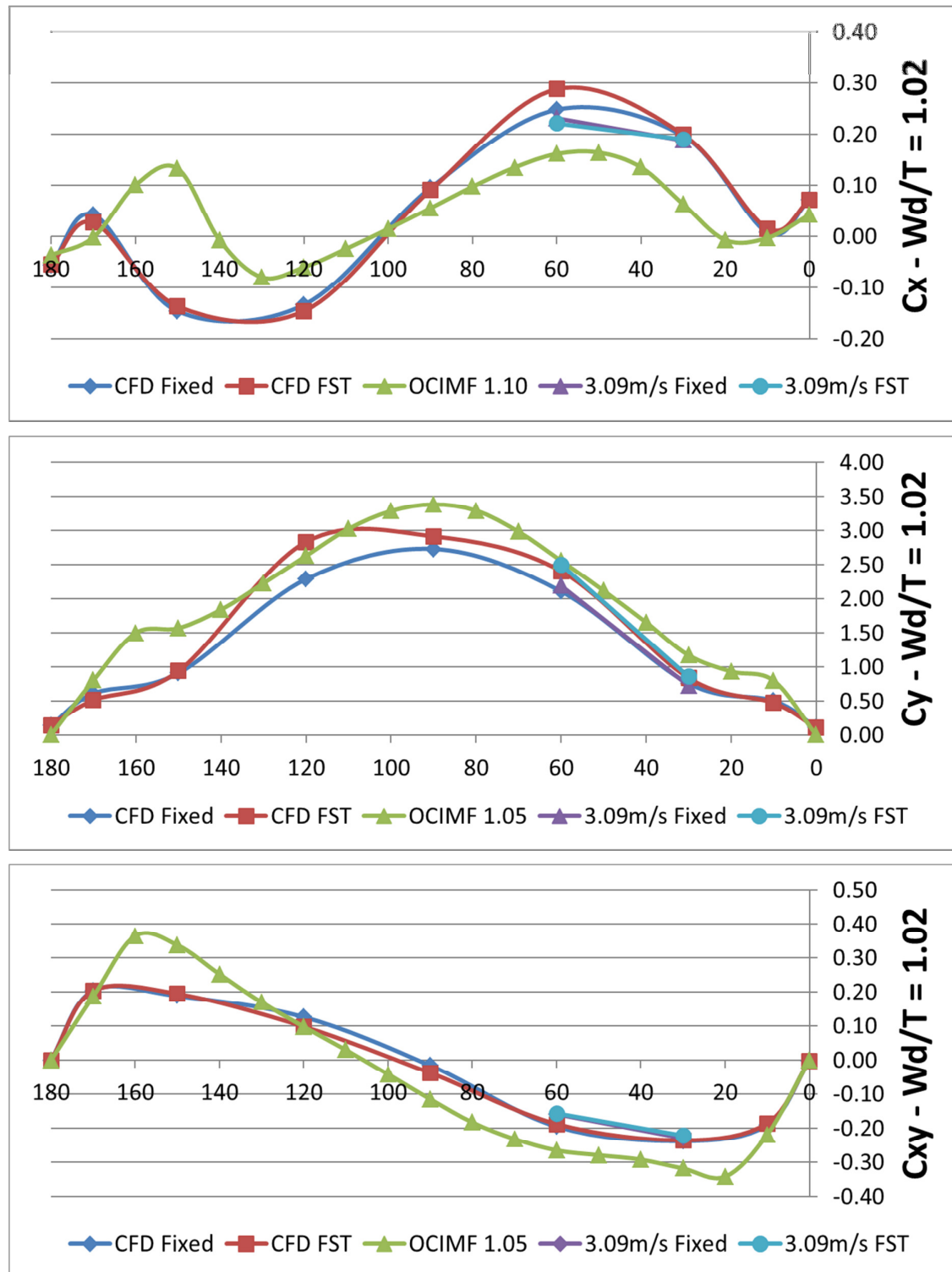


Figure 14: Current sensitivity - Wd/T 1.02 results

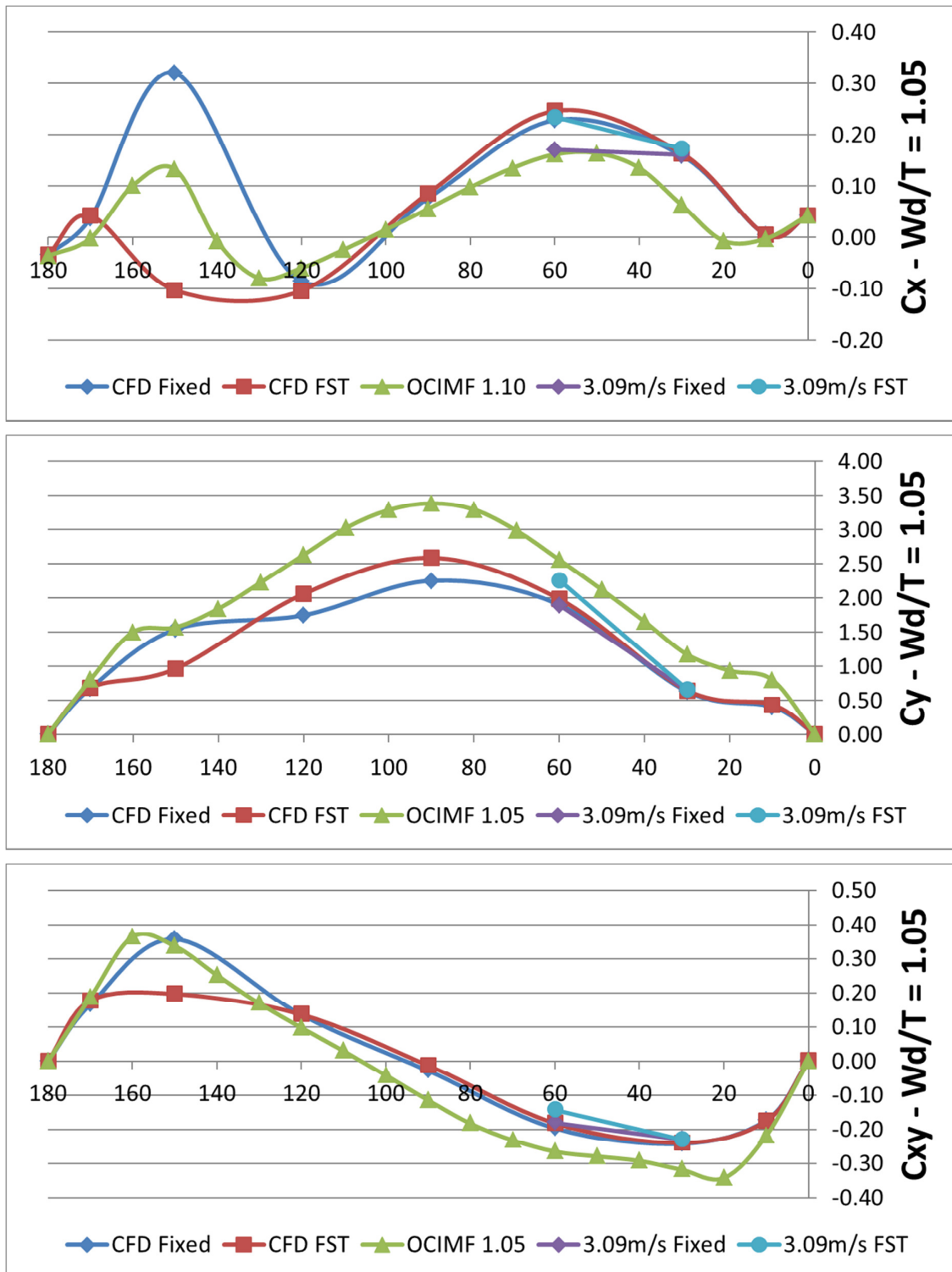


Figure 15: Current sensitivity - Wd/T 1.05 results

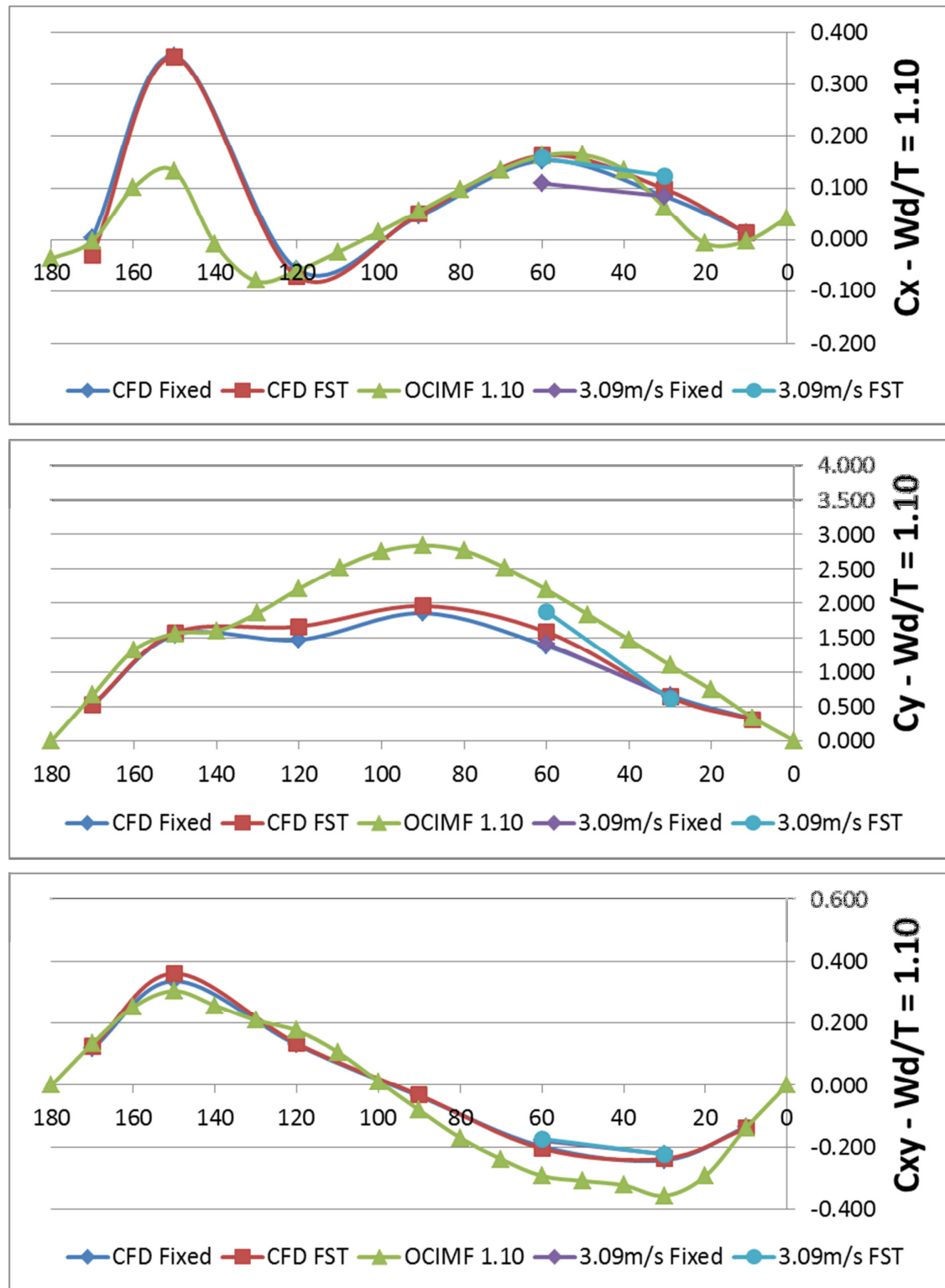


Figure 16: Current sensitivity - Wd/T 1.10 results

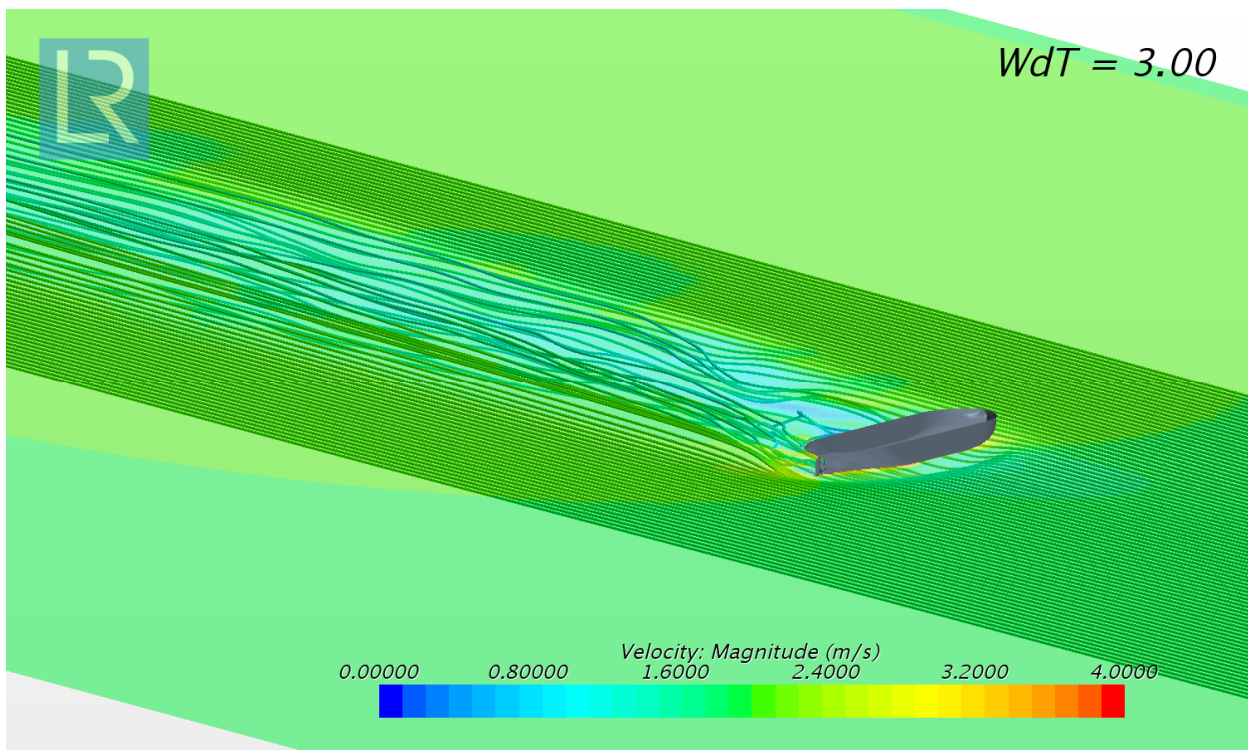


Figure 17: Discussion – Streamlines, Laden, Wd/T 3.00, 60 degrees

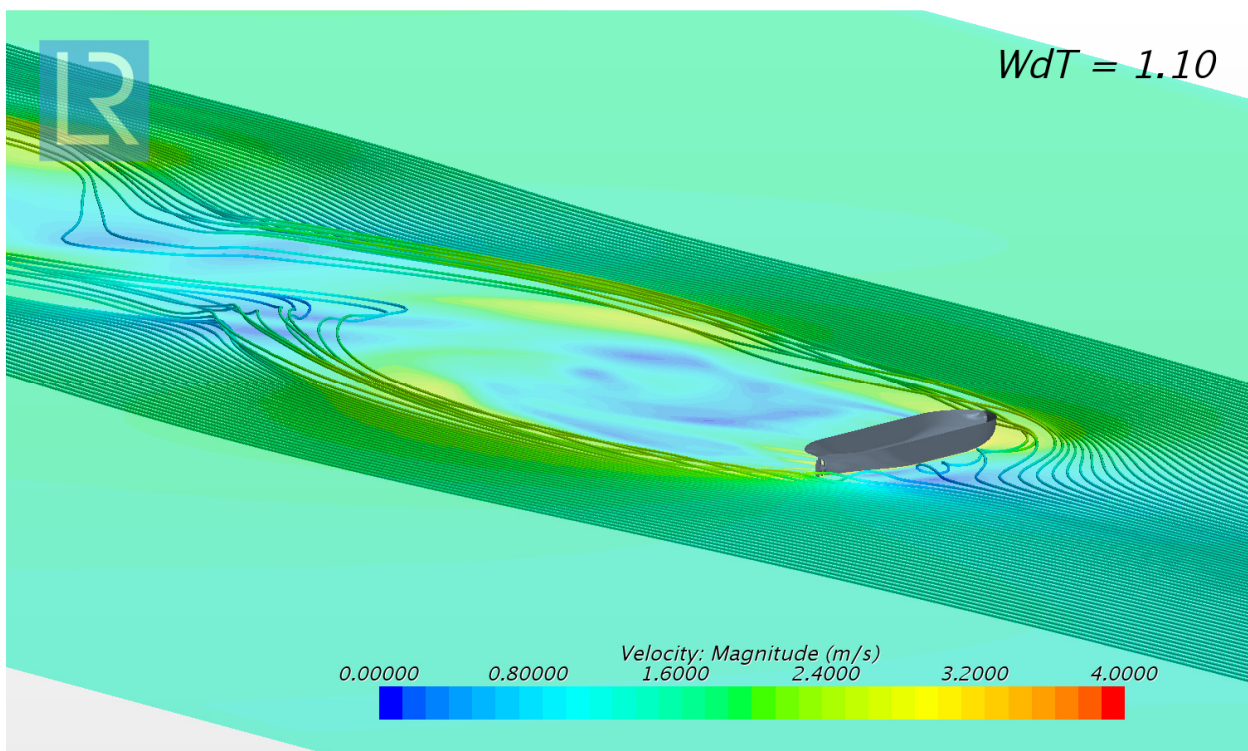


Figure 18: Discussion - Streamlines, Laden 17m, Wd/T 1.10, 60 degrees

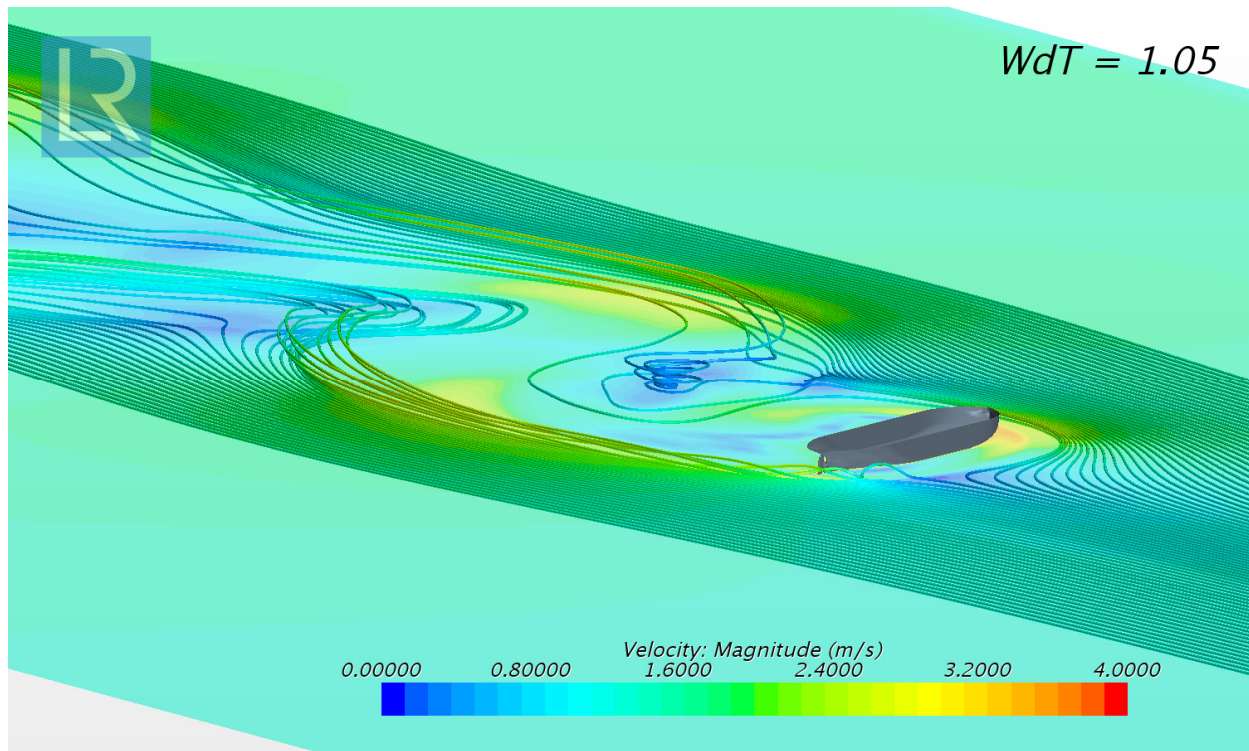


Figure 19: Discussion - Streamlines, Laden, Wd/T 1.05, 60 degrees

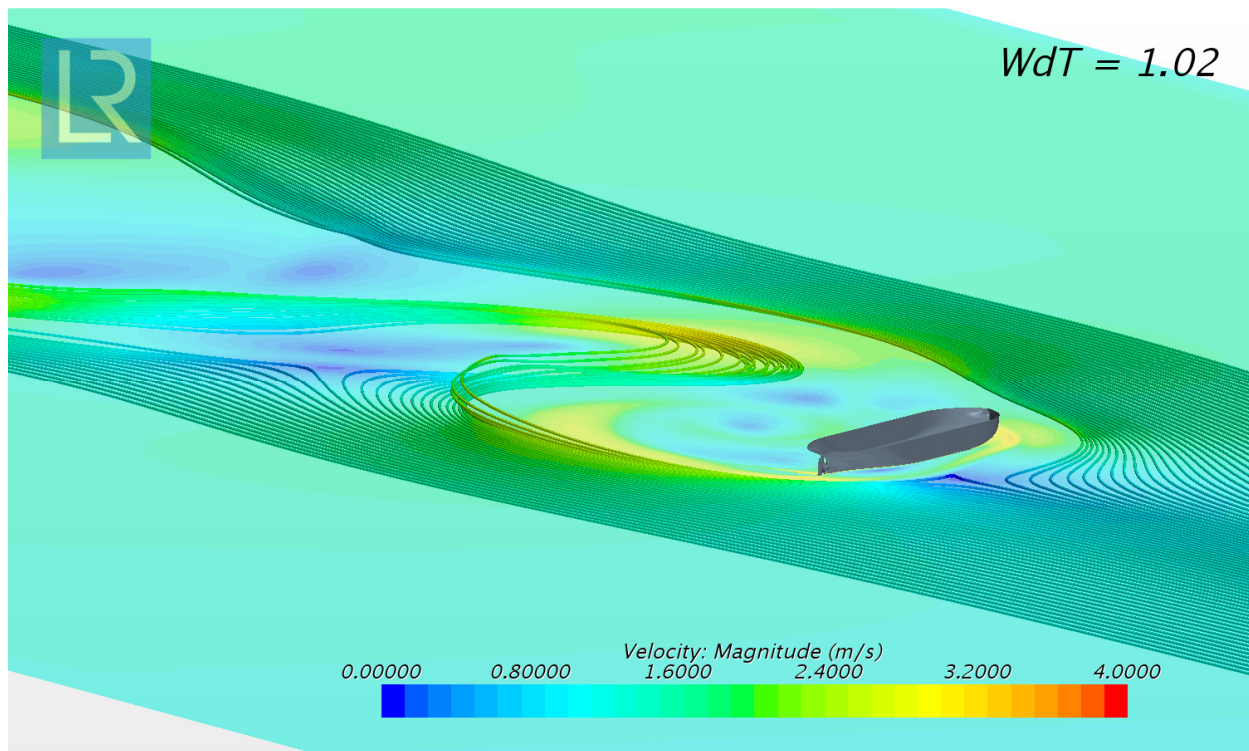


Figure 20: Discussion - Streamlines, Laden, Wd/T 1.02, 60 degrees

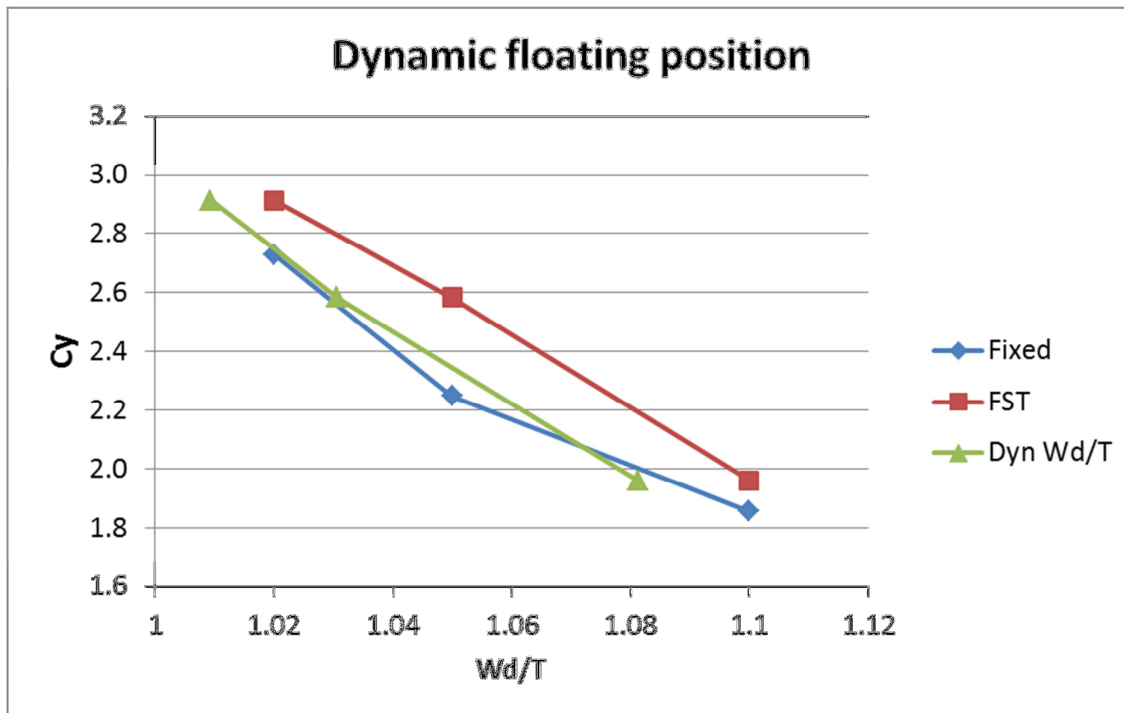


Figure 21: Discussion - Dynamic floating position, Laden, 90 degrees

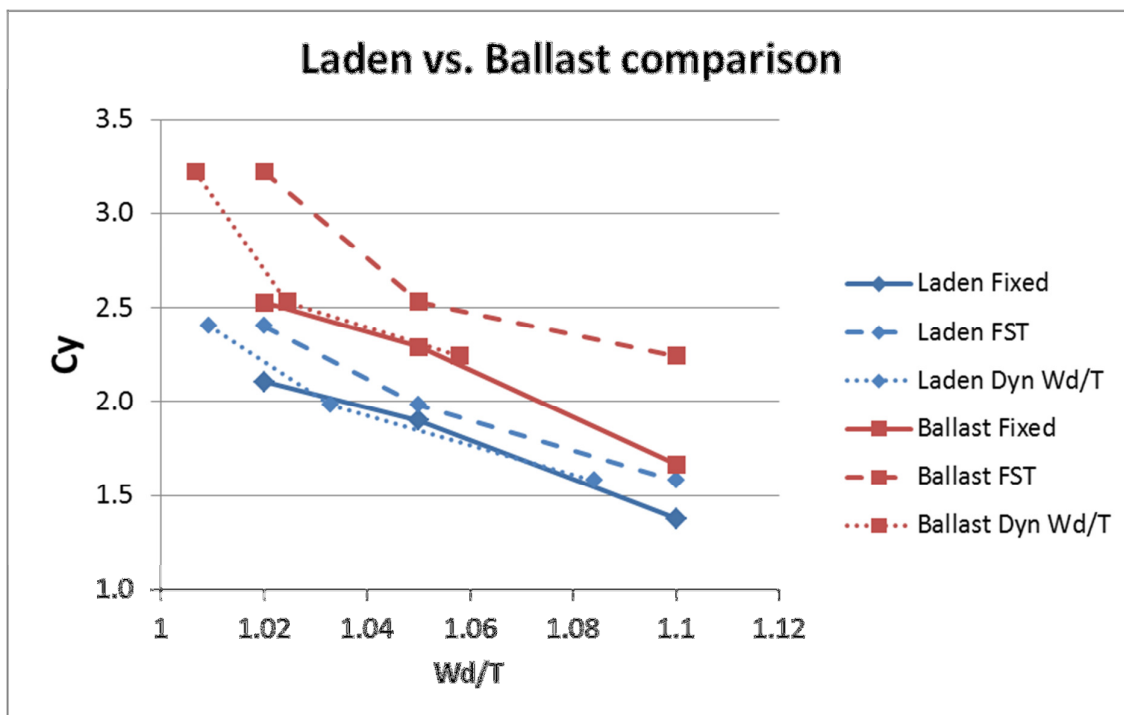


Figure 22: Discussion - Laden vs. Ballast comparison

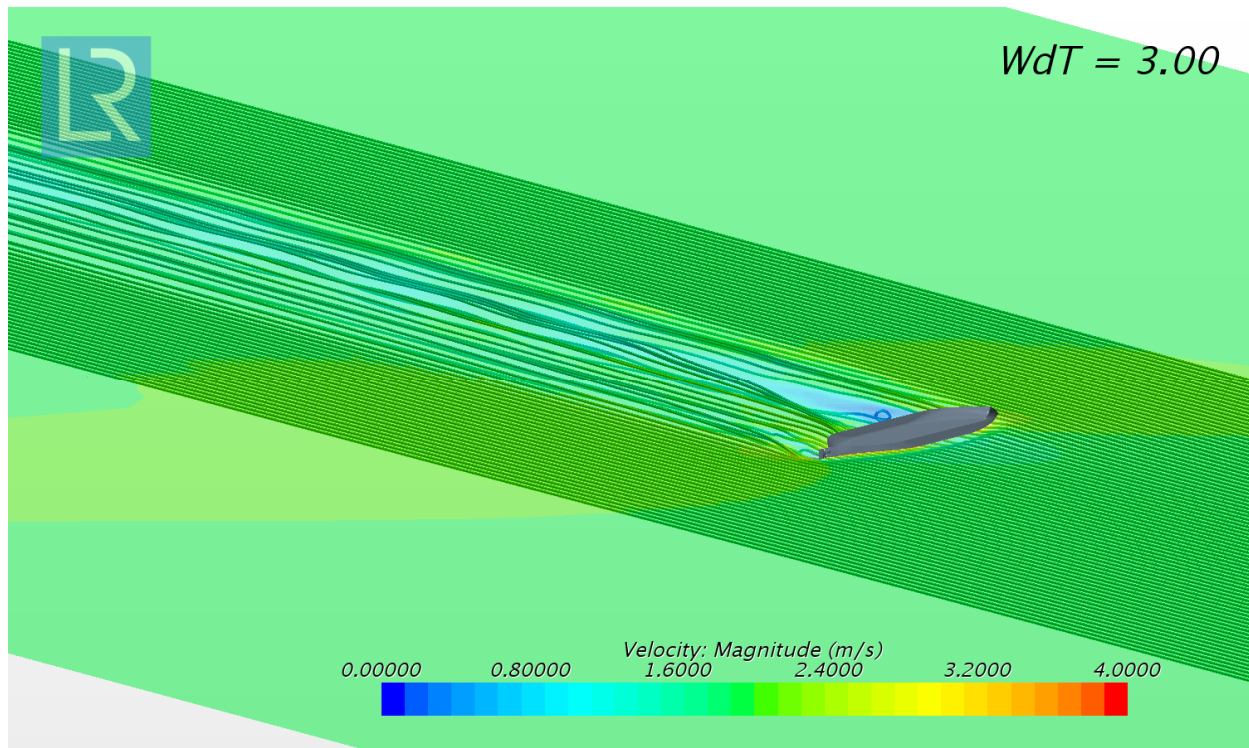


Figure 23: Discussion - Streamlines, Ballast, Wd/T 3.00, 60 degrees

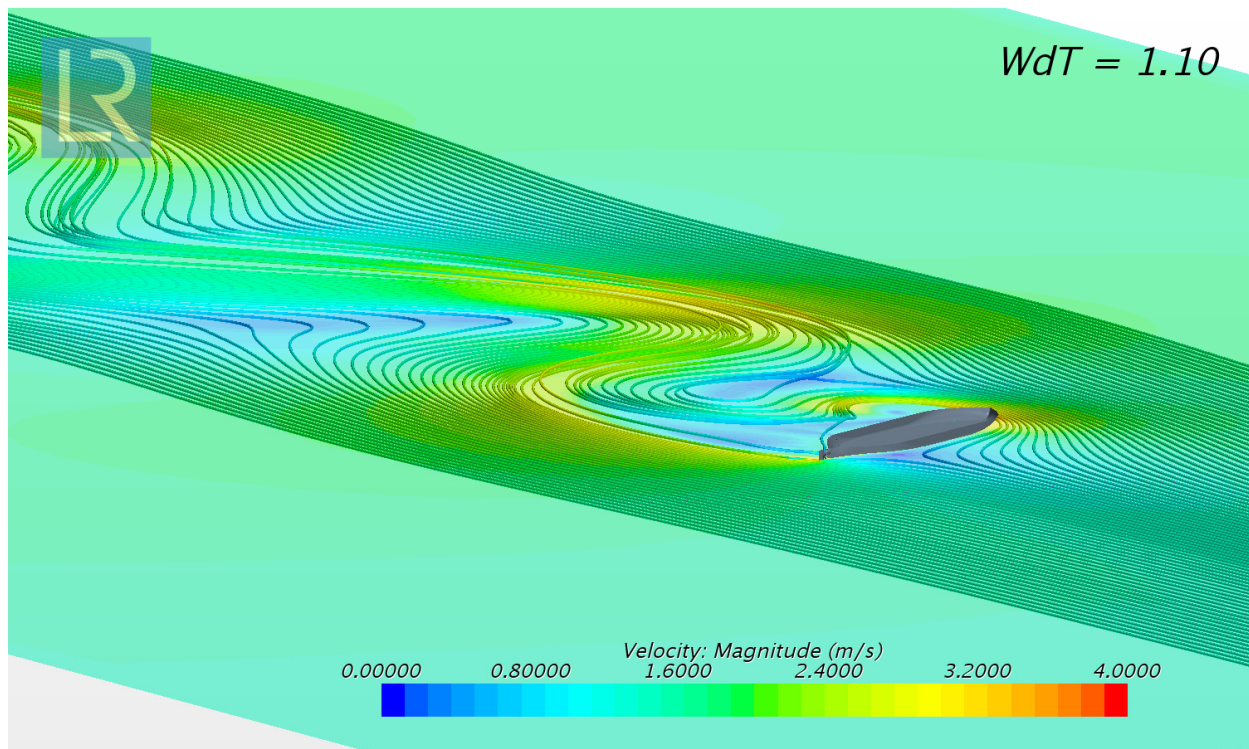


Figure 24: Discussion - Streamlines, Ballast, Wd/T 1.10, 60 degrees

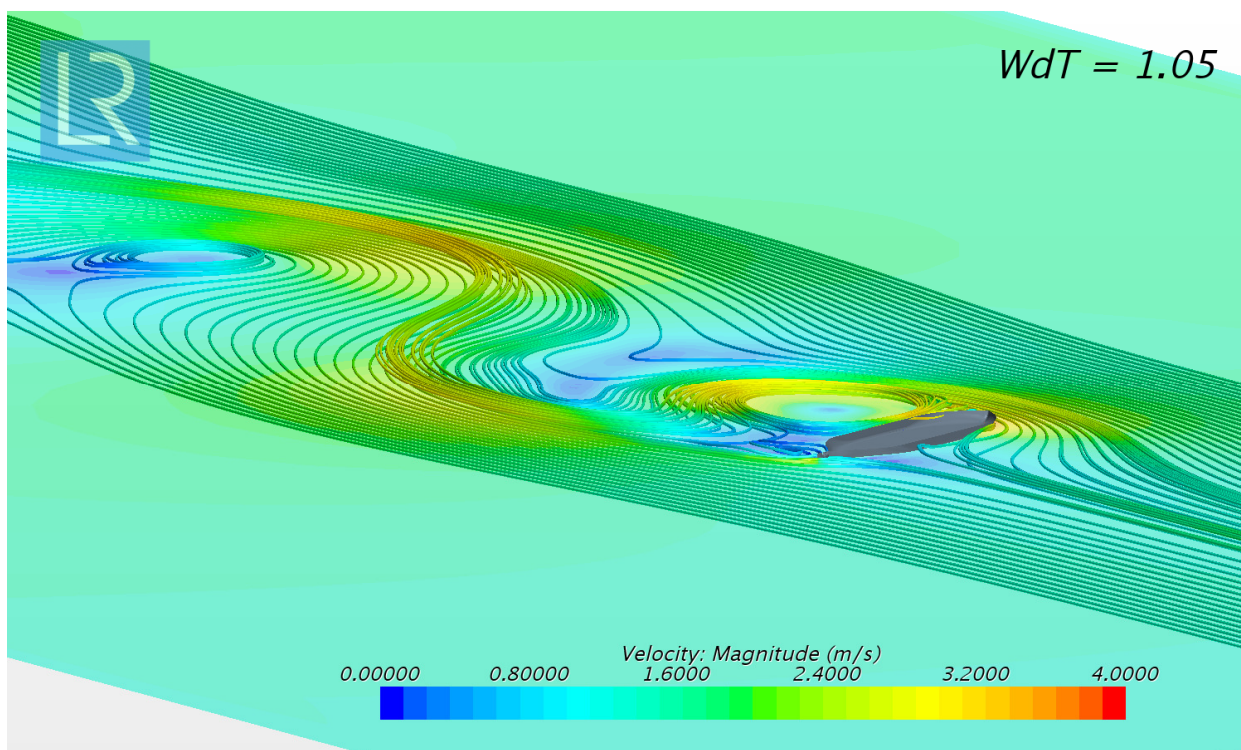


Figure 25: Discussion - Streamlines, Ballast, Wd/T 1.05, 60 degrees

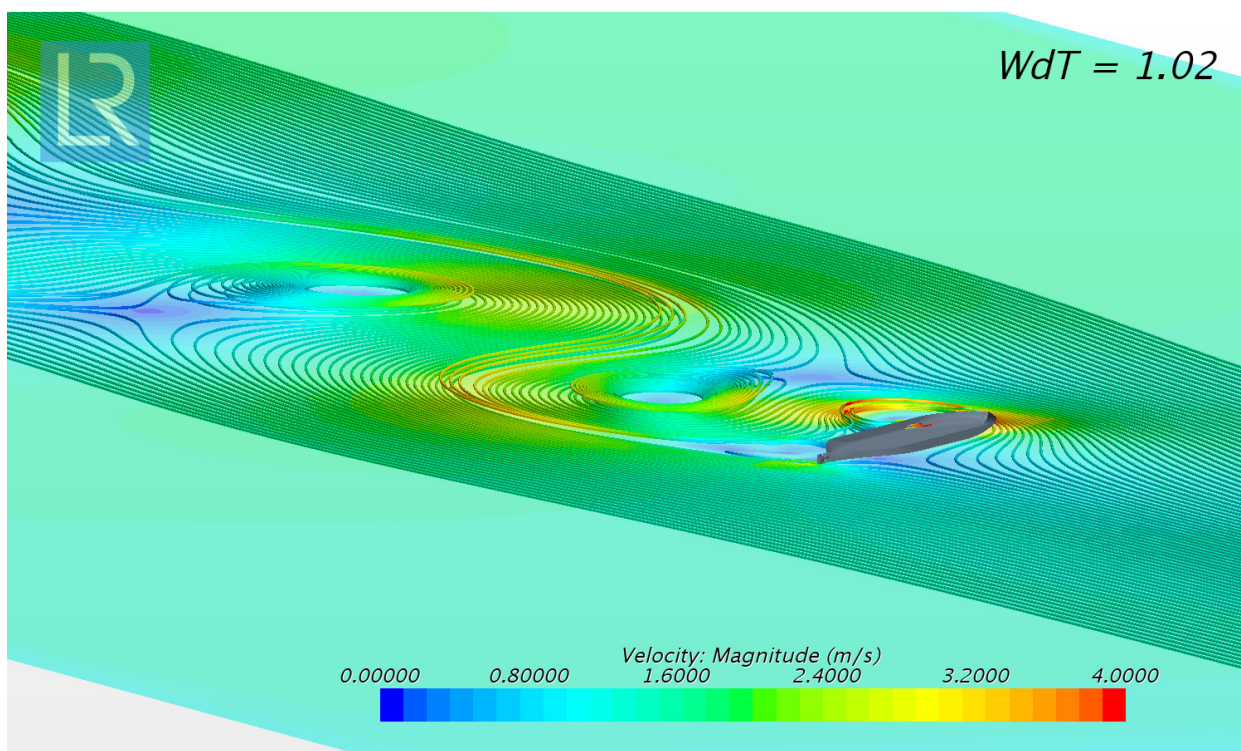


Figure 26: Discussion - Streamlines, Ballast, Wd/T 1.02, 60 degrees

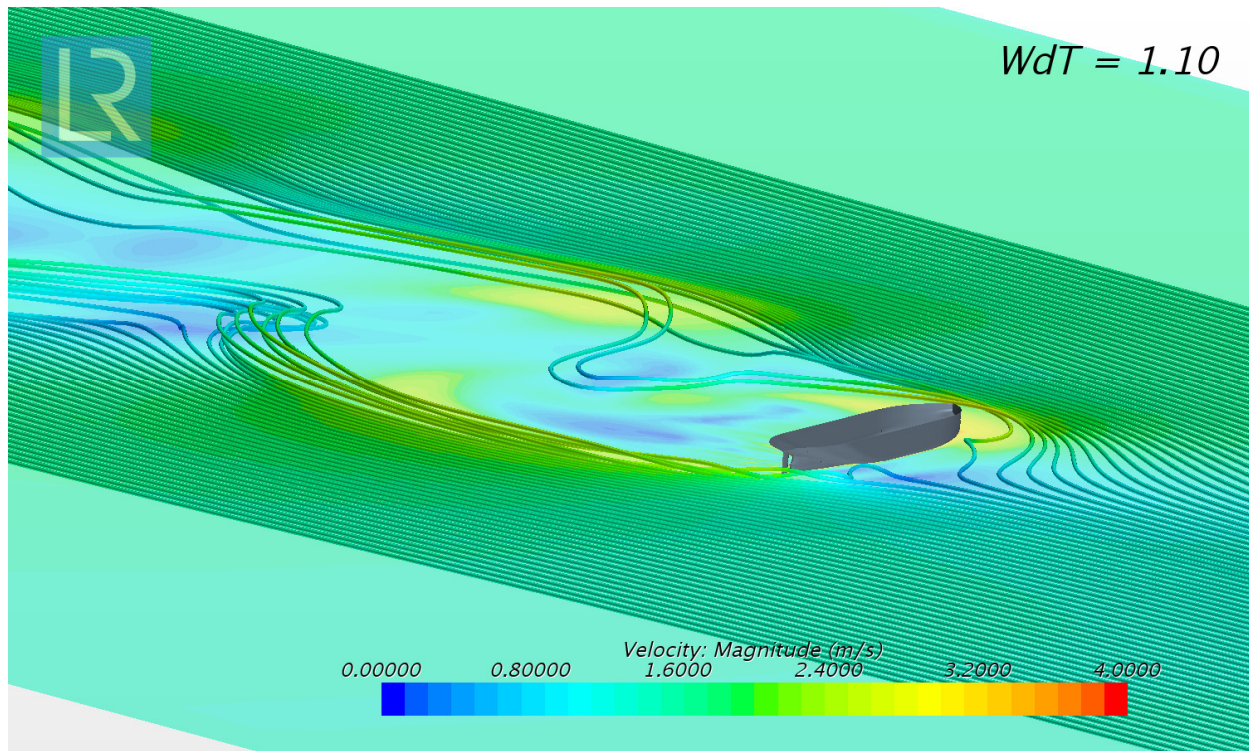


Figure 27: Discussion - 50kDWT, Laden 12.5m, Wd/T 1.10, 60 degrees, Streamlines

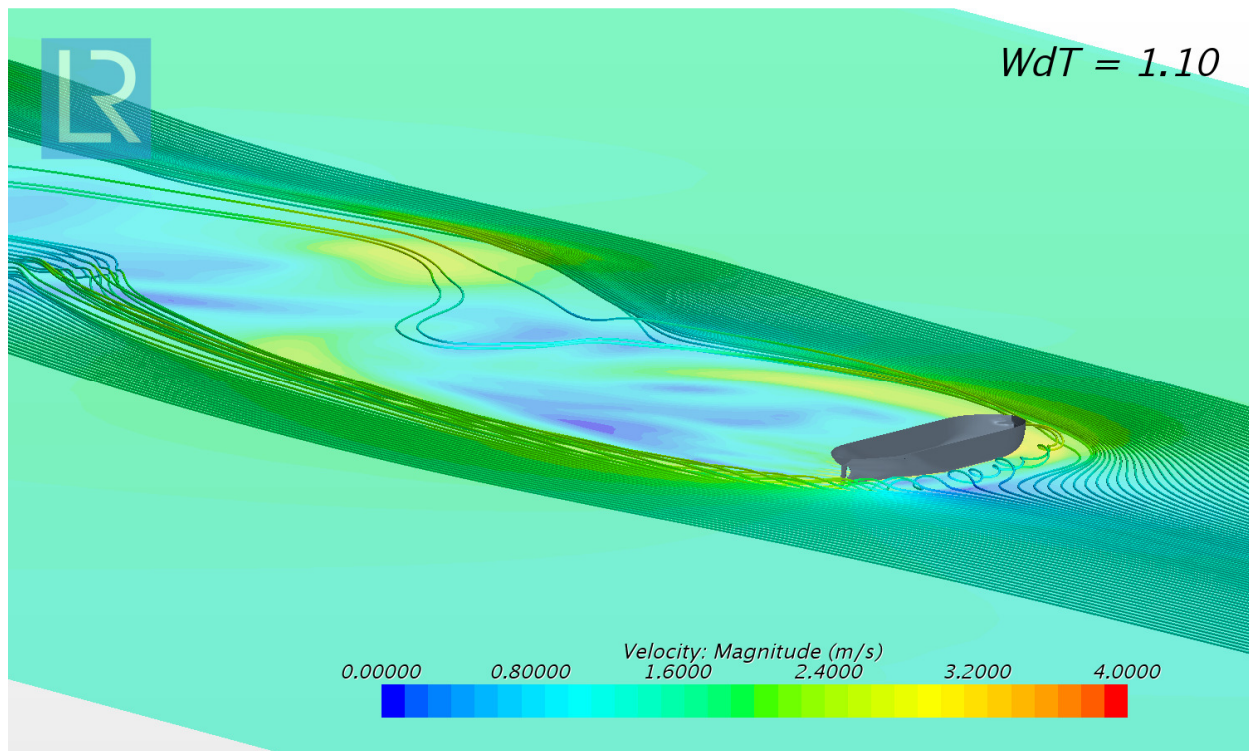


Figure 28: Discussion - 300kDWT, Laden 22.6m, Wd/T 1.10, 60 degrees, Streamlines

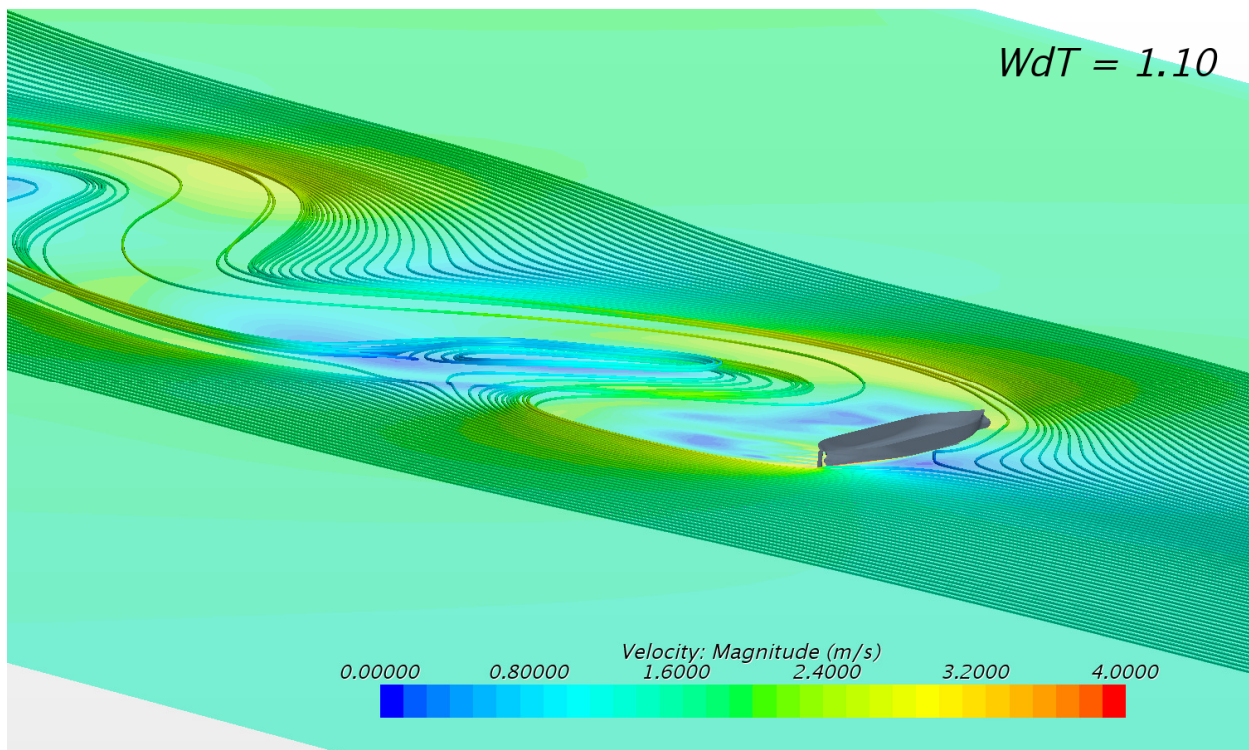


Figure 29: Discussion - LNG, Laden 11.8m, Wd/T 1.10, 60 degrees, Streamlines

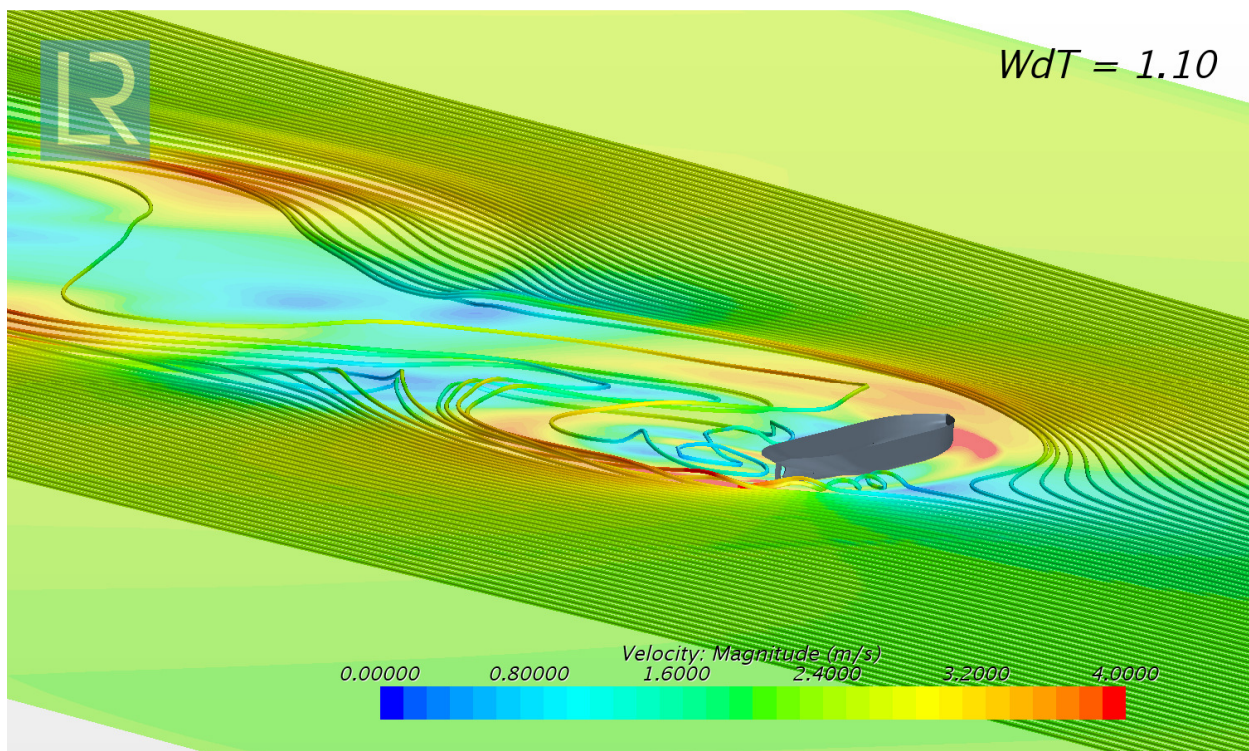


Figure 30: Discussion - 50kDWT, 3.09m/s, Laden 12.5m, Wd/T 1.10, 60 degrees, Streamlines

Erik A.J. Vroegrijk

Specialist Hydrodynamics

Tel: +44(0)33 0414 0494

Mob : +44 (0)7805 746394

Email: erik.vroegrijk@lr.org

Chris Craddock

Manager Fluid Dynamics

Tel: +44(0)33 0414 0481

Mob: +44 (0) 7816 334309

Email: chris.craddock@lr.org

Lloyd's Register EMEA, TID
Lloyd's Register Global Technology Centre
Southampton Boldrewood Innovation Campus
Burgess Road, Southampton
SO16 7QF

www.lr.org

Lloyd's Register Group Limited, its subsidiaries and affiliates and their respective officers, employees or agents are, individually and collectively, referred to in this clause as 'Lloyd's Register'. Lloyd's Register assumes no responsibility and shall not be liable to any person for any loss, damage or expense caused by reliance on the information or advice in this document or howsoever provided, unless that person has signed a contract with the relevant Lloyd's Register entity for the provision of this information or advice and in that case any responsibility or liability is exclusively on the terms and conditions set out in that contract.

Lloyd's Register and variants of it are trading names of Lloyd's Register Group Limited, its subsidiaries and affiliates.
Copyright © Lloyd's Register EMEA. 2017. A member of the Lloyd's Register group.